An MC-SCF/MP2 Study of the Photochemistry of 2,3-Diazabicyclo[2.2.1]hept-2-ene: Production and Fate of Diazenyl and Hydrazonyl Biradicals

Naoko Yamamoto,[†] Massimo Olivucci,*[,‡] Paolo Celani,[†] Fernando Bernardi,[‡] and Michael A. Robb*[,†]

Contribution from the Department of Chemistry, King's College, London, Strand, London WC2R 2LS, U.K., and Dipartimento di Chimica "G. Ciamician" dell'Universita di Bologna, Via Selmi 2, 40126 Bologna, Italy

Received May 27, 1997

Abstract: A CAS-SCF/MP2 study of the photolysis of 2,3-diazabicyclo[2.2.1]hept-2-ene (DBH) has been carried out with use of a 6-31G* basis. The S_1 (n−π*), T_1 (n−π*), and T_2 (π−π*) reaction paths for deazetization (via α C−N cleavage) and rearrangement reaction to azirane (via β C−C cleavage) have been investigated along with the associated reaction pathways for cyclization and rearrangement of the photoproduct, 1,3-cyclopentanediyl biradical. It is shown that singlet and triplet photoexcited DBH evolve along a network of 18 ground and excited-state intermediates, 17 transition structures and 10 "funnels", where internal conversion (IC) or intersystem crossing (ISC) occurs. Three cyclic excited-state species are reached following evolution from the Franck−Condon region: two metastable singlet (n−π*) and triplet (n−π*) species and a stable excited state ^{3}(n−π*)−^{3}(π−π*) intermediate. It is demonstrated that the singlet ^{1}(n−π*) intermediate can decay directly to S_0 or undergo ISC to generate the ^{3}(n−π*)−^{3}(π−π*) intermediate or/and the ^{3}(n−π*) intermediate. The ^{3}(n−π*) intermediate can directly decay to the T_1 diazenyl biradical or undergo IC to generate the ^{3}(n−π*)−^{3}(π−π*) intermediate. Finally, the much more stable ^{3}(n−π*)−^{3}(π−π*) intermediate cannot be converted to the other excited state intermediates but can only react via either α C−N and β C−C cleavage. Our computed energetics suggest that the ^{3}(n−π*)−^{3}(π−π*) intermediate is the best candidate for the experimentally observed transient triplet intermediate.

1. Introduction

The 2,3-diazabicyclo[2.2.1]hept-2-ene (DBH) species (Scheme 1, structure **A**) and its derivatives denitrogenate photochemically (and thermally) through a α C−N cleavage to yield 1,3-cyclopentanediyl biradicals (structures **C** and **D**).[1−3] The biradical C usually cyclizes to housanes (structure **E**) or it may undergo rearrangement to form cyclopentenes (structure **F**) via 1,2 hydrogen shift.[3] Photochemical transformations of DBH derivatives (e.g. as structure **A′**) other than denitrogenation have been observed in a few cases. When certain prerequisites (e.g., increased ring stiffness and strain effects) are met,[4] β C−C cleavage occurs. Increased ring stiffness due to the additional etheno bridge and simultaneous allylic stabilization of the resulting biradical results in the concurrent formation of azirane (structure **J′**)[4a−c] and the usual housane products in DBH. (Diazoalkane products are also observed in other similar reactions via β C−C cleavage [4 e].)

The photoproducts resulting from photoinduced α and β cleavage are presently rationalized via formation of the two corresponding singlet (S_0) or/and triplet (T_1) diazenyl ($\mathbf{D}_{\sigma\sigma}$) and hydrazonyl ($\mathbf{D}_{\sigma\pi}$) biradicals (structures **B** and **G′**, respectively). These intermediates can thus be regarded as the "hubs" of DBH photochemistry. While this seems confirmed by substantial experimental evidence (see below), very little is known about the excited-state origin and nature of these species or the detailed mechanism of their production.

A broad range of photophysical and photochemical measurements on DBH (including absorption, emission, and fluorescence excitation spectra, and the pressure-dependent yields for fluorescence and photodissociation) were first made by Solomon and co-workers.[5] Their results showed that, unlike its acyclic counterparts, vapor-phase DBH exhibits a structured rather than a diffuse $S_1 \rightarrow S_0$ absorption spectrum, and fluorescence from its S_1 (n−π*) state can be observed with a quantum yield of 1.4×10^{-2}. The emission, absorption, and excitation maxima at 29540 ± 10 cm^{-1} (84.5 kcal mol^{-1}) was assigned to the (0−0) transition. Gas-phase DBH photodissociates from its S_1 state with a quantum yield of ∼1. However, DBH again differs from the acyclics by retaining its high photodissociative yield in solution. The triplet state is also found to be dissociative both in the gas phase and in solution.

In the period since the report of Solomon et al., a number of experiments have been carried out on this system and its

[†] King's College.
[‡] Universita di Bologna.

(1) (a) Engel, P. S. *Chem. Rev.* **1980**, *80*, 99. (b) Adam, W.; De Lucchi, O. *Angew. Chem., Int. Ed. Engl.* **1980**, *19*, 762.
(2) Clark, W. D. K.; Steel, C. *J. Am. Chem. Soc.* **1971**, *93*, 6347.
(3) Adam, W.; Oppenlander, T.; Zang, G. *J. Org. Chem.* **1985**, *50*, 3303.
(4) (a) Adam, W.; Nau, W. M.; Sendelbach, J.; Wirtz, J. *J. Am. Chem. Soc.* **1993**, *115*, 12571. (b) Adam, W.; Nau, W. M.; Sendelbach, J. *J. Am. Chem. Soc.* **1994**, *116*, 7049. (c) Adam, W.; Fragale, G.; Klapstein, D.; Nau, W. M.; Wirtz, J. *J. Am. Chem. Soc.* **1995**, *117*, 12578. (d) Adam, W.; De Lucchi, O. *J. Am. Chem. Soc.* **1980**, *102*, 2109. (e) Adam, W.; Gillaspey, W. D.; Peters, E.-M.; Peters, K.; Rosenthal, R. J.; von Schnering, H. G. *J. Org. Chem.* **1985**, *50*, 580.
(5) Solomon, B. S.; Thomas, T. F.; Steel, C. *J. Am. Chem. Soc.* **1968**, *90*, 2249.

S0002-7863(97)01733-2 CCC: $15.00
Published on Web 02/28/1998

Scheme 1

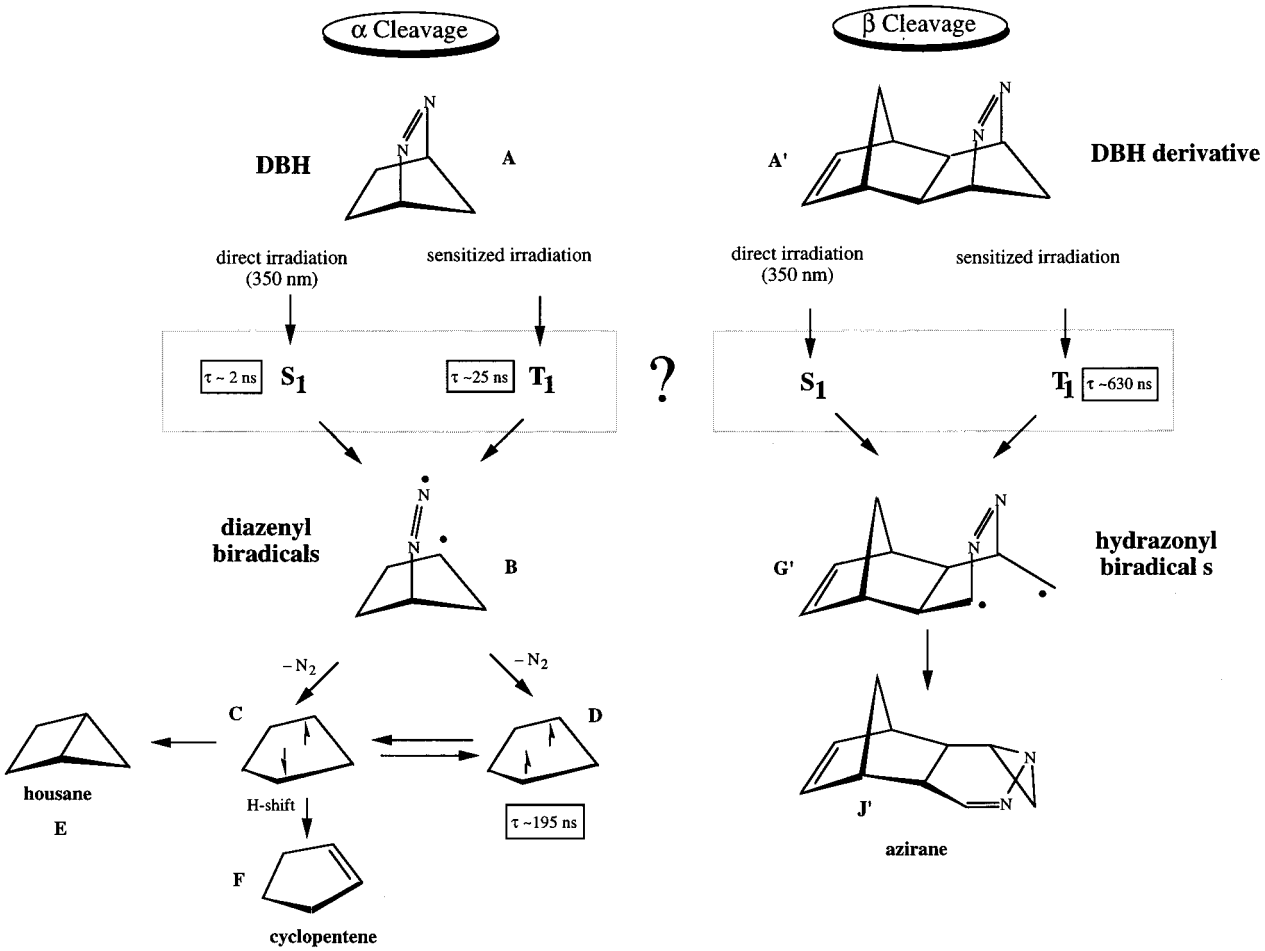

derivatives.[1−4,6−12] Research in this area has been centered on the following: (a) determining whether the two C−N bonds break in a single step or in two,[3,6−10] (b) identifying and characterizing any reaction intermediates, and understanding the roles played by various electronic states in photolysis,[3,10] (c) intramolecular dynamics of denitrogenation,[11,12] and (d) the question of α C−N versus β C−C bond scission.[4a−c]

In the past few years, the controversial problem of synchronous or asynchronous α C−N bond cleavage in the conventional photolysis of DBH appears to have been resolved in favor of the latter mechanism.[3,6−10] Adam and co-workers carried out a detailed mechanistic study of the transformations of unsubstituted and alkyl-substituted DBH induced by various types of activation modes (pyrolysis, photosensitized electron transfer (PET), 185-nm, laser-jet, and 350-nm photolysis).[3,10] Pyrolysis and conventional direct 350-nm photolysis of DBH yielded bicyclo[2.1.0]pentanes (structure **E** in Scheme 1) and very small amounts of cyclopentenes (structure **F**) while benzophenone-sensitized 350-nm photolysis of DBH only gave the first product. PET, benzophenone-sensitized laser-jet, and 185-nm photolysis of the DBH led to significant quantities of cyclopentene derivatives. On the basis of these observations, it has been suggested that a diazenyl biradical (structure **B**) resulting in a stepwise one-bond cleavage mechanism serves as a common intermediate in both pyrolysis and 350-nm photolysis of DBH while a two-bond cleavage leading directly to the 1,3-cyclopentanediyl biradicals (structures **C** and **D**) is involved in 185-nm photolysis.

Weisman et al.[8] studied the gas-phase photochemistry of DBH excited to the S_1 state at 338.5 nm (84.5 kcal mol^{-1}) using time-resolved coherent anti-Stokes Raman spectroscopy (CARS) on the nanosecond time scale. Their measured vibrational distribution of the unrelaxed nitrogen photoproduct, when compared to those formed from azomethane, shows a very similar vibrational state distribution but a significantly cooler rotational distribution. To explain this cool rotational distribution of N_2, they have also suggested that fragmentation occurs from an excited state of the diazenyl biradical (structure **B** in Scheme 1) which has a linear C−N−N bond angle. Their fluorescence lifetime measurements show the S_1 (n−π*) state to undergo collision-free decay with a characteristic lifetime of slightly more than 2 ns (see Scheme 1). Time-resolved CARS measurements have revealed that molecular nitrogen is produced from a precursor, originally attributed to the linear diazenyl radical **B**,

(6) Bauer, S. H. *J. Am. Chem. Soc.* **1969**, *91*, 3688.
(7) Adams, J. S.; Burton, B. K.; Andrews, R. B.; Weisman, R. B.; Engel, P. S. *J. Am. Chem. Soc.* **1986**, *108*, 7935.
(8) Adams, J. S.; Weisman, R. B.; Engel, P. S. *J. Am. Chem. Soc.* **1990**, *112*, 9115.
(9) Simpson, C. J. S. M.; Wilson, G. J.; Adam, W. *J. Am. Chem. Soc.* **1991**, *113*, 4728.
(10) (a) Adam, W.; Denninger, U.; Finzel, R.; Kita, F.; Platsch, H.; Walter, H.; Zang, G. *J. Am. Chem. Soc.* **1992**, *114*, 5027. (b) Adam, W.; Hossel, P.; Hummer, W.; Platsch, H.; Wilson, R. M. *J. Am. Chem. Soc.* **1987**, *109*, 7570. (c)Adam, W.; Grabowski, S.; Wilson, R. M. *Acc. Chem. Res.* **1990**, *23*, 165−172.
(11) (a) Lyons, B. A.; Pfeifer, J.; Carpenter, B. K. *J. Am. Chem. Soc.* **1991**, *113*, 9006. (b) Peterson, T. H.; Carpenter, B. K. *J. Am. Chem. Soc.* **1992**, *114*, 766. (c) Carpenter, B. K. *Acc. Chem. Res.* **1992**, *25*, 520. (d) Lyons, B. A.; Pfeifer, J.; Peterson, T. H.; Carpenter, B. K. *J. Am. Chem. Soc.* **1993**, *115*, 2427.
(12) (a) Sorescu, D. C.; Thompson, D. L.; Raff, L. M. *J. Chem. Phys.* **1994**, *101*, 3729. (b) Sorescu, D. C.; Thompson, D. L.; Raff, L. M. *J. Chem. Phys.* **1995**, *102*, 7910.

whose lifetime is approximately 25 ns, and that a precursor of the bicyclopentane photoproduct (**E**) has a lifetime of 195 ns. From these observations, they have concluded that S_1 excitation of vapor-phase DBH produces 1,3-cyclopentanediyl biradicals only in their ground triplet state (**D**), although in solution photolysis, a singlet channel (**A** → **B** → **C** → **E**) seems to dominate.

Buchwalter and Closs[13] exploited the potential energy surface of bicyclic azoalkanes to form biradicals by photolyzing matrix-isolated DBH and taking ESR spectra of the resulting triplet 1,3-cyclopentanediyl (shown as **D** in Scheme 1).[13] Their temperature-dependent studies of the ESR signals from the triplet 1,3-cyclopentanediyl biradical (structure **D**) provided an estimate of its activation barrier (2.3 ± 0.2 kcal mol^{-1}) for decay into bicyclopentane (shown as **E** in Scheme 1). The topology of the singlet 1,3-cyclopentanediyl potential energy surface has been the subject of controversy. While Benson-type thermochemical calculations suggest a minimum (structure **C**) on the singlet surface with a well depth of 5 kcal mol^{-1},[14] Buchwalter and Closs[13] proposed that the singlet 1,3-cyclopentanediyl is unstable and exists as a transition state. A study by Goodman and Herman[15] using the time-resolved photoacoustic calorimetry also suggests that the singlet biradical is a transition sate or a very shallow minimum. Schaefer et al. carried out a theoretical study of the singlet and triplet potential energy surfaces for 1,3-cyclopentanediyl using a DZ+d basis set at the SCF and CISD level of theory.[16a] Their results indicate that there is a shallow local minimum on the singlet surface.

More recently, Adam and co-workers have reported the first direct spectroscopic charcterization of the long-lived triplet state of the DBH derivative (*anti*-hexahydro-1,4:5,8-dimethanophthalazine, shown as **A′** in Scheme 1)[4a] and the mechanistic implication on its photoreactivity.[4b] Their investigation of the direct and triplet-sensitized photolysis of this molecule shows exceptional photochemical and photophysical properties. On direct irradiation, azoalkane **A′** does not only give the expected housane (i.e., obtained via denitrogenation and radical recombination) through α C−N bond cleavage and subsequent denitrogenation but also yields azirane (structure **J′**) via β C−C bond cleavage. From the increased formation of the heterocycle (**J′**) on triplet sensitization, Adam et al. have concluded that the azirane (**J′**) is derived from the long-lived triplet state of the azoalkane by β C−C bond cleavage with subsequent cyclization. From the temperature dependence of the direct and sensitized photoreactions of azoalkane **A′**, they estimated the relative activation energies to be ≥3.3 and ≥10.5 kcal mol^{-1} for α C−N scission from the singlet and triplet states and ≥7.9 kcal mol^{-1} for the β C−C bond cleavage from the triplet. Adam and co-workers have also obtained first phosphorescence spectra of fused derivatives of DBH and assigned this long-lived triplet state to the ^{3}(n−π*) state.[4c] However, parent DBH failed to show any phosphorescence emission under the same conditions.

Despite a vast amount of experimental data, the only theoretical study of photochemistry of DBH is the work of Robertson and Simons.[16b] This study was limited to documentation of energetics associated with the ^{1,3}(n−π*) transition states and the diazenyl radical, and no attempt was made to investigate ISC or IC processes. In this paper, we present a comprehensive study of the potential energy surfaces and reaction paths of the singlet (S_0, S_1) and triplet (T_1, T_2) states associated with the photolysis of DBH. These data are used to get insight into the rather complex reaction network sustaining the photochemical production of housane and azirane from DBH and its derivatives. *As we will see subsequently, this reaction network comprises: eighteen energy minima, seventeen transition structures, three conical intersection funnels, and seven triplet/singlet crossing funnels.* (see ref 17a for a review that discusses how these topological features are defined)

We have investigated the, essentially unknown, excited-state intermediate region marked "?" in Scheme 1. According to our results, production of the biradicals (the diazenyl and hydrazonyl) controlling the photochemistry of DBH and its derivatives occurs according to Scheme 2a via formation of *three* different excited-state intermediates.

Two of these intermediates belong to the triplet manifold but have different molecular structure and electronic nature (n−π* **XX** and "mixed" n−π*−π−π* **XIX**, respectively). The third intermediate is a singlet n−π* structure **XV**. The triplet "mixed" n−π*−π−π* intermediate is the only one which, potentially, undergoes β cleavage and can be produced by direct irradiation (via sequential intersystem crossing (ISC) and internal conversion (IC)) or by sensitized irradiation (via IC from the triplet n−π* state). As illustrated in Scheme 2b, our results also reveal that there are three main initial molecular deformation modes controlling the production of the excited-state intermediates. Formation of both the triplet and the singlet n−π* intermediates is induced via a N═N−C bending deformation of the ground-state DBH structure. In contrast formation of the "mixed" n−π*−π−π* intermediate involves C−N═N−C torsional motion coupled with −N═N− bond stretching.

Thus our objectives are (a) to elucidate how the three intermediates marked in Scheme 2 are initially formed in direct and sensitized irradiation conditions, (b) to elucidate how the diazenyl and hydrazonyl biradicals are generated via α and/or β cleavage of these structures (c) to rationalize the differences in product distribution (i.e. the ratios of housane (structure **E** in Scheme 1) to cyclopentene (structure **F**)) in denitrogenation of DBH induced by various activation modes, and (d) to explain the temperature dependence of denitrogenation to azirane (structure **J′**) ratios in the direct and triplet-sensitized photolysis of DBH derivatives (e.g. structure **A′**).

2. Computational Details

The strategy for carrying out excited state mechanistic studies has recently been reviewed,[17a] so we mention only a few essential details here. It has been demonstrated, via extensive computational work,[18] that the photochemical reaction mechanism consistent with the experimental knowledge can be formulated by using four different mechanistic elements: (a) energy minima, (b) transition states (saddle points), (c) singlet/singlet and triplet/triplet conical intersections (real crossings between states of the same spin-multiplicity), and (d) singlet/triplet crossings. Conical intersections are regarded as the main locus of internal conversion (IC) while triplet/singlet crossings are the main locus of intersystem crossings (ISC). Very recently new computational results on n−π* excited states and biradical

(13) (a) Buchwalter, S. L.; Closs, G. L. *J. Am. Chem. Soc.* **1975**, *97*, 3857. (b) Buchwalter, S. L.; Closs, G. L. *J. Am. Chem. Soc.* **1979**, *101*, 4688.

(14) (a) Beadle, P. C.; Golden, D. M.; King, K. D.; Benson, S. W. *J. Am. Chem. Soc.* **1972**, *94*, 2943. (b) O'Neal, H. E.; Benson, S. W. *Int. J. Chem. Kinet.* **1970**, *2*, 423. (c) Luo, Y. R.; Benson, S. W. *J. Phys. Chem.* **1989**, *93*, 3304.

(15) Herman, M. S.; Goodman J. L. *J. Am. Chem. Soc.* **1988**, *110*, 2681.

(16) (a) Sherrill, C. D.; Seidl, E. T.; Schaefer, H. F., III *J. Phys. Chem.* **1992**, *96*, 3712. (b) Robertson M. J.; Simons, J. *J. Phys. Chem. A* **1997**, *101*, 2379.

(17) (a) Bernardi, F.; Olivucci, M.; Robb, M. A. *Chem. Soc. Rev.* **1996**, *25*, 321. (b) Klessinger, M. *Angew. Chem., Int. Ed. Engl.* **1995**, *34*, 549−551.

Scheme 2

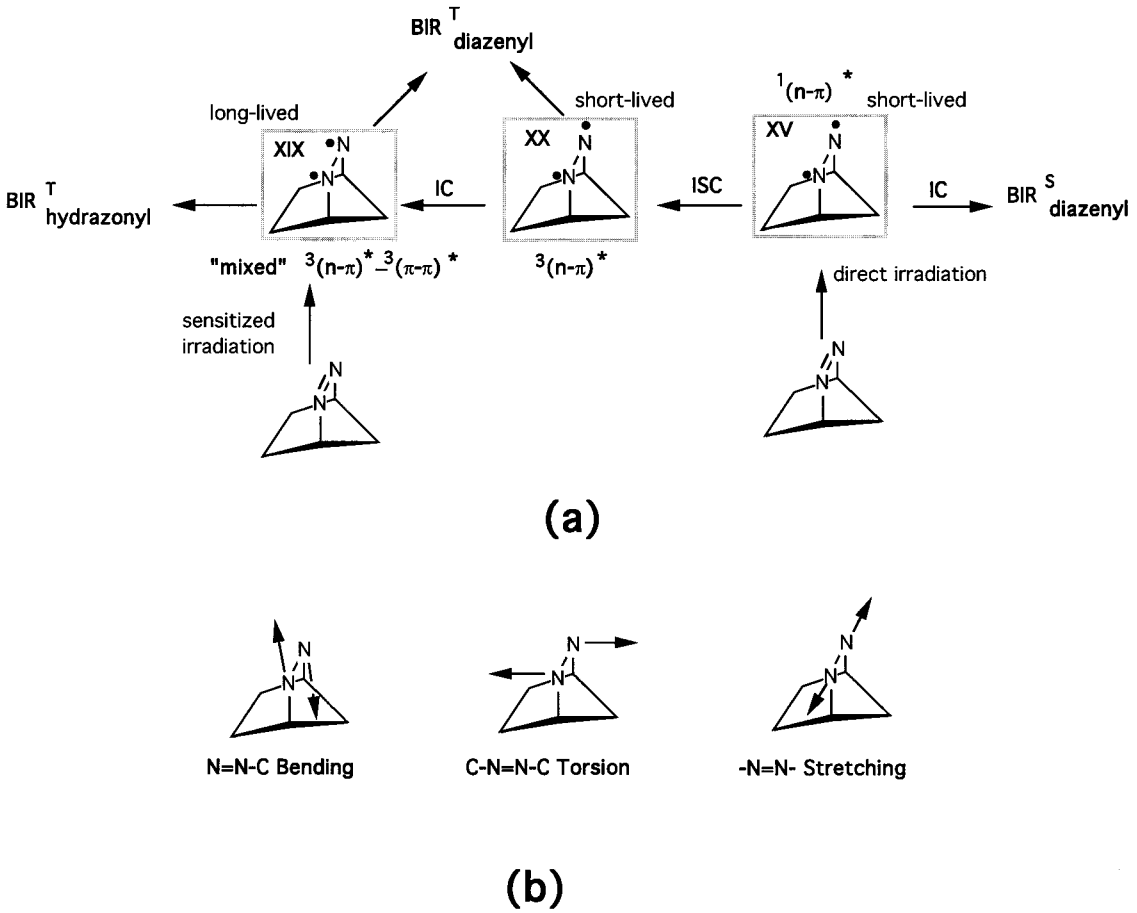

systems (such as α,β and β,γ enones)[18f,h] have revealed the existence of a rather unconventional mechanistic element, which is represented by a biradical structure where different singlet and triplet potential energy surfaces (either of n−π* or π−π* electronic structure) are nearly degenerate. These points can be the locus of both IC and ISC and can be seen as a pair of intersecting conical intersections (i.e. one T_1/T_2 and one S_0/S_1 intersections).

All of the CAS-SCF results presented in this paper have been produced by using the MC-SCF program distributed in *Gaussian 94*[20] with a 6-31G* basis. A multireference MP2 algorithm[21] that has been implemented in Gaussian was used to correct the energetics for dynamic correlation. Geometry optimizations were performed at the CASSCF level and the MP2 correction (no frozen core or virtual orbitals) was added to produce improved energetics (without re-optimization of the geometry). The location of the surface crossings corresponding to conical intersection points and singlet−triplet crossings has been carried out by using the method[19] that is also available in the *Gaussian* package. Spin−orbit coupling constants have been calculated in an approximation by using scaled nuclear charges[22] and one-electron integrals of the H_{LS} operator. Analytical frequency calculations were carried out by using the direct CP-MCSCF (coupled-perturbed-MCSCF) method that has been documented elsewhere.[23]

The choice of active space in our computations requires some comment. To describe the synchronous fragmentation to N_2 from the ground state, one needs both pairs of C−N σ and σ* orbitals and 4 orbitals from N_2 (π and π* and two *n* orbitals), i.e., 10 electrons in 8 orbitals, as shown in Figure 1a. For studying asynchronous α-cleavage reaction from DBH excited states one only needs one of the two α C−N σ and σ* orbital pairs and one *n* orbital plus the π system (6 electrons in 5 orbitals). However, in the region of second C−N scission, the

(18) (a) Palmer, I. J.; Ragazos, I. N.; Bernardi, F.; Olivucci M.; Robb, M. A. *J. Am. Chem. Soc.* **1993,** *115*, 673. (b) Celani, P.; Ottani, S.; Olivucci, M.; Bernardi, F.; Robb, M. A. *J. Am. Chem. Soc.* **1994,** *116*, 10141−10151. (c) Celani, P.; Garavelli, M.; Ottani, S.; Bernardi, F.; Robb, M. A.; Olivucci, M. *J. Am. Chem. Soc.* **1995**, *117*, 11584−11585. (d) Palmer, I. J.; Ragazos, I. N.; Bernardi, F.; Olivucci, M.; Robb, M. A. *J. Am. Chem. Soc.* **1994**, *116*, 2121−2132. (e) Reguero, M.; Olivucci, M.; Bernardi, F.; Robb, M. A. *J. Am. Chem. Soc.* **1994**, *116*, 2103−2114. (f) Wilsey, S.; Bearpark, M. J.; Bernardi, F.; Olivucci, M.; Robb, M. A. *J. Am. Chem. Soc.* **1996**, *118*, 176−184. (g) Yamamoto, N.; Bernardi, F.; Bottoni, A.; Olivucci, M.; Robb, M. A.; Wilsey, S. *J. Am. Chem. Soc.* **1994**, *116*, 2064−2074. (h) Wilsey, S.; Bearpark, M. J.; Bernardi, F.; Olivucci, M.; Robb, M. A. *J. Am. Chem. Soc.* **1996**, *118*, 4469−4479. (i) Celani, P.; Bernardi, F.; Olivucci, M.; Robb, M. A. *J. Chem. Phys.* **1995**, *102*, 5733−5742. (l) Bearpark, M. J.; Bernardi, F.; Clifford, S.; Olivucci, M.; Robb, M. A.; Smith, B. R.; Vreven, T. *J. Am. Chem. Soc.* **1996**, *118*, 169−175.

(19) (a) Ragazos, I. N.; Robb, M. A.; Bernardi, F.; Olivucci, M. *Chem. Phys. Lett.* **1992**, *197*, 217. (b) Yarkony, R. D. *J. Phys. Chem.* **1993**, *97*, 4407. (c) Bearpark, M. J.; Robb, M. A.; Schlegel, H. B. *Chem. Phys. Lett.* **1994**, *223*, 269.

(20) *Gaussian '94*, Revision B, Frisch, M. J.; Trucks, G. W.; Schlegel, H. B.; Gill, P. M. W.; Johnson, B. G.; Robb, M. A.; Cheeseman, J. R.; Keith, T.; Petersson, G. A.; Montgomery, J. A.; Raghavachari, K.; Al-Laham, M. A.; Zakrzewski, V. G.; Ortiz, J. V.; Foresman, J. B.; Cioslowski, J.; Stefanov, B. B.; Nanayakkara, A.; Challacombe, M.; Peng, C. Y.; Ayala, P. Y.; Chen, W.; Wong, M. W.; Andres, J. L.; Replogle, E. S.; Gomperts, R.; Martin, R. L.; Fox, D. J.; Binkley, J. S.; Defrees, D. J.; Baker, J.; Stewart, J. P.; Head-Gordon, M.; Gonzalez, C.; Pople, J. A.; Gaussian, Inc.: Pittsburgh, PA, 1994.

(21) McDouall, J. J. W.; Peasley, K.; Robb, M. A. *Chem. Phys. Lett.* **1988**, *148*, 183.

(22) Koseki, S.; Schmidt, M. W.; Gordon, M. S. *J. Phys. Chem.* **1992**, *96*, 10768.

(23) Yamamoto, N.; Vreven, T.; Robb, M. A.; Frisch, M. J.; Schlegel, H. B. *Chem. Phys. Lett.* **1996**, *250*, 373−378.

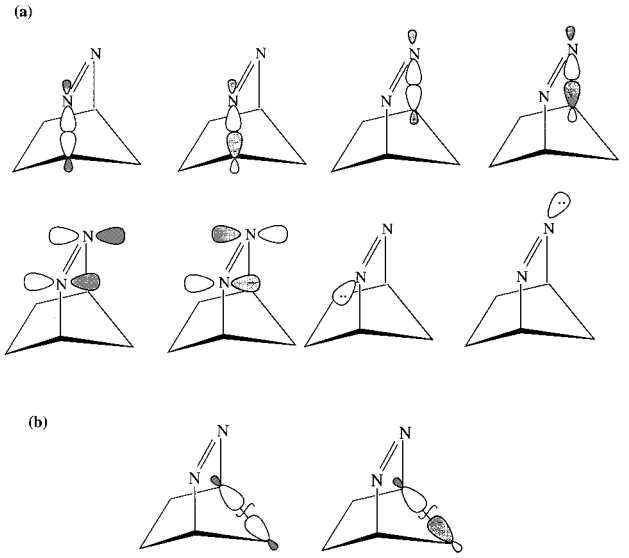

Figure 1. Active space used for studying the (a) α C−N cleavage reaction and the (b) β C−C cleavage reaction.

full 8 active orbitals must be used. To describe the C−C β scission reaction path, the α C−N σ and σ^* orbitals are redundant (i.e. they have occupancies of 2 and 0), though one needs the β C−C σ and σ^* pair in the active space (Figure 1b). The inclusion of redundant orbitals changes the energy slightly because these orbitals will make a small contribution to the dynamic correlation; however, the MC-SCF convergence is seriously degraded. The use of different active spaces for different regions of the potential energy surface for geometry optimization makes the comparison of energies subject to a small error because nondynamic and dynamic correlation effects are not strictly separable. However, at the MP2 level these differences are minimized. For two computations with different active spaces, where the differences correspond to orbitals with occupancies near 2 or 0, the CAS-SCF/MP2 results should be very similar. The small difference can be explained from the fact that the dynamic correlation arising from the redundant orbitals is included to infinite order in the large active space, rather than to second order in the reduced active space.

It is appropriate at this point to comment on the reliability and accuracy of the methods used in this work. We can calibrate our CAS/MP2 results on the ground state calculations against results of the experimental studies of thermal decomposition of DBH which have been carried out extensively in the past few years.[11,12,24] As we shall demonstrate in the next section, we find the barrier for the asynchronous thermal decomposition of DBH to be 35.5 kcal mol^{-1} (29.9 kcal mol^{-1} with zero-point energy correction). This compares well with the experimental value of 36.0 kcal mol^{-1}.[11d] Our vertical excitation energy and the (0−0) energy gap are 93.8 and 80.9 kcal mol^{-1}, respectively, although Solomon et al. has observed the coincidence of the emission, absorption, and excitation maxima at 84.5 kcal mol^{-1} which has been assigned to the (0−0) band.[5]

3. Results and Discussion

In the following subsections we shall document the main features of the ground (S_0) and excited state (S_1, T_1, and T_2) surfaces of *parent* DBH associated with the photochemical denitrogenation, through α C−N cleavage, and the formation of azirane via β C−C cleavage (however, the production of azirane from parent DBH has never been observed so these are "model computations"). This will be accomplished in four subsections. In subsections (**i**) and (**ii**) we document the mechanism of production of the diazenyl and hydrazonyl biradicals, respectively. The molecular and electronic structures and evolution of the diazenyl and hydrazonyl radicals will be documented in subsection (**iii**). Finally, in subsection (**iv**) we will discuss the competition between cyclization and rearrangement in the primary product of nitrogen extrusion: the 1,3-cyclopentanediyl diradical.

To conserve space the geometrical parameters for all computed molecular structures can be found in the Supporting Information and are referred to as Figures S1−S11 in the following text and tables. The corresponding energetic data are collected in Table 1. The results of these computations generate a rather complex reaction network that is summarized in eq 1.

Schematically, the DBH molecule is initially transformed via three different excited-state intermediates (framed structures). The singlet (n−π^*) intermediate **XV** has one short and one long C−N bond generated via an anti-symmetric bending of the two −C−N═N− angles of DBH (see Scheme 2b). Almost the same structural features are found in the triplet (n−π^*) intermediate **XX**. In contrast the triplet mixed (n−π^*)−(π−π^*) intermediate **XIX** has a highly twisted −CN═NC− moiety. This last intermediate is the only one potentially capable of producing the hydrazonyl biradical and can be generated via both sensitized and direct irradiation (probably via intermediate **XX**). In contrast, the diazenyl biradical can be produced by all three intermediates. The (n−π^*) intermediates seem to produce the exo diazenyl biradical while intermediate **XIX** produces the endo diazenyl biradical.

The detailed reaction pathways for the various processes illustrated in eq 1 are given in Schemes 3−5, 7, and 8. The energy values (framed values) reported in these schemes are relative to the ground-state reactant DBH and are given in kilocalories per mole.

(i) Direct and Sensitized Photochemical Production of Diazenyl Biradical Intermediates ($^{1,3}D_{\sigma\sigma}$). We shall now describe the reaction paths on the S_1, T_1, and T_2 surfaces leading to the $^{1,3}D_{\sigma\sigma}$ biradicals (shown as **B** in Scheme 1). A schematic representation of the computed pathways for the production of the diazenyl biradical is shown in Scheme 3. There are three facets of this problem: (a) the competition between production of singlet biradicals (via IC from S_1) and triplet biradicals (via $S_1 \rightarrow T_2$ ISC) upon direct irradiation, (b) the nature of the singlet and triplet excited-state species detected experimentally, and (c) the relationship between the reaction paths for direct and triplet-sensitized photolysis.

(a) Direct Irradiation and Evolution from S_1. Let us turn our attention to the decay mechanism from the S_1 (n−π^*) state prepared by *direct* irradiation. The Franck−Condon region of the S_1 (n−π^*) surface has the characteristics of a transition state. In particular, at a geometry very close to the S_0 equilibrium structure (structure **A**), we have characterized an S_1 (n−π^*) transition state (Scheme 4a, structure **XIV**, Figure S4a) which lies ca. 90 kcal mol^{-1} above the reactant. The normal coordinate corresponding to the imaginary frequency (347*i* cm^{-1}) involves the antisymmetric bending of the two ∠NNC angles (see Scheme 2b). If one follows this transition vector one finds a shallow S_1 (n−π^*) minimum (structure **XV**, Figure S4b) ca. 10 kcal mol^{-1} below the Franck−Condon structure.

This S_1 minimum corresponds to the excited state "reactant"

(24) (a) Allred, E. L.; Smith, R. L. *J. Am. Chem. Soc.* **1969**, *91*, 6766. (b) Roth, W. R.; Martin, M. *Justus Liebigs Ann. Chem.* **1967**, *702*, 1. (c) Roth, W. R.; Martin, M. *Tetrahedron Lett.* **1967**, *47*, 4695.

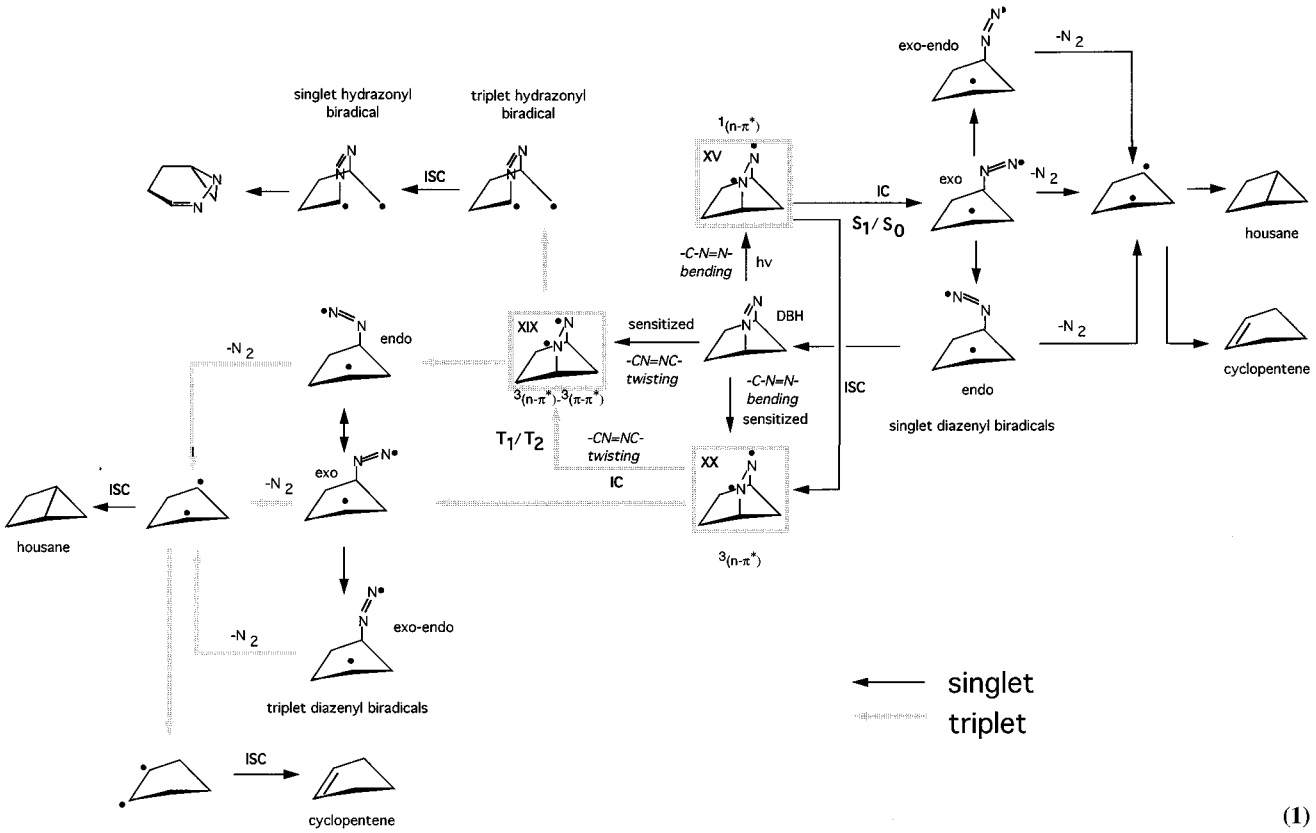

(1)

and evolves toward either efficient IC or ISC. As reported in Scheme 3 at 4.8 kcal mol^{-1} above this minimum, there exists a transition state for α C−N ring-opening (structure **XVII**, Figure S4d). A minimum energy path computation (MEP) from this transition state leads to an acyclic structure corresponding to a 4-fold (S_0, S_1, T_1, T_2) crossing (structure **I**). At this multiple funnel, decays to T_1 and S_0 are both possible in principle. However, the latter is more likely to occur since IC via conical intersection is fully efficient. Therefore, if the molecule enters the region of this crossing along the S_1 (n−π*) reaction coordinate, it will decay to the S_0 surface and will produce S_0 diazenyl biradicals. The evolution of the DBH molecular structure along the MEP also suggests that the exo conformation of the diradical is most likely to be populated (see also subsection **iii**) due to the large momentum acquired during excited-state motion.

At just 0.1 kcal mol^{-1} above the S_1 minimum (N−N = 1.30 Å and longer C−N = 1.59 Å) we have located a S_1 (n−π*)/T_2 (π−π*) crossing point (structure **XVI**, Figure S4c). The molecular structure of this crossing (N−N = 1.32 Å and longer C−N = 1.56 Å) is shown in Figure S4b together with its gradient difference vector (see ref 17a for a discussion). It is apparent that in order to reach the crossing the system must slightly expand the −N=N− bond length and decrease the asymmetry in the ∠NNC bendings. Since the spin−orbit coupling (SOC) is found to be relatively large (20.0 cm^{-1}), the ISC is predicted to be favorable. The relatively large SOC value between S_1 (n−π*) and T_2 (π−π*) is consistent with the fact that the transition from S_1 (n−π*) to T_2 (π−π*) DBH is associated with the situation where the spin flip is coupled with the electron flip between a p orbital along one axis and an *n* orbital along an orthogonal axis with a concomitant large orbital angular momentum change.

While our computations suggest that the S_1/T_2 structure (**XVI**) is 0.1 kcal mol^{-1} higher than the S1 min (**XV**) and that the S_1 α cleavage TS (structure **XVII**) is 4.9 kcal mol^{-1} higher, in the S_1/T_2 crossing region the S_1 and T_2 surfaces are almost parallel. Thus the optimized (i.e., the gradient is below the threshold) S_1/T_2 crossing structure still has a residual 5 kcal mol^{-1} gap between S_1 and T_2 (Table 1). Thus the only safe conclusion is that ISC and α cleavage must be competitive processes.

Notice that our computed barrier compares well with the experimental activation energy (≥3.3 kcal mol^{-1})[4b] of S_1 α C−N cleavage for the DBH derivative (structure **A′**). Further, the presence of the small barrier for the C−N cleavage and the S_1/T_2 surface crossing accounts for the observed low fluorescence quantum yield (1.4×10^{-2}) from S_1.[5]

(b) Sensitized Irradiation and Decay from T_1. The decay channel for the triplet-sensitized photolysis is closely related to the S_1 decay path discussed above and illustrated in Scheme 3. In the Franck−Condon region, T_2 has (π−π*) character and lies ca. 34 kcal mol^{-1} (CAS−SCF value) above T_1 which has (n−π*) character. As the structure of the molecule gets distorted from the Franck−Condon geometry, the ^{3}(π−π*) and ^{3}(n−π*) states become strongly mixed so that it becomes difficult to distinguish between the two triplet states, especially at structures where the C−N=N−C bridge is twisted. In other words, the electronic structures of the T_1 and T_2 states become a combination of (π−π*) and (n−π*) configurations.

Near the triplet (n−π*) energy minimum (structure **XX** in Scheme 4b) we have located the lowest energy point on the conical intersection between the (π−π*) and (n−π*) triplet states (see structure **XVIII** in Schemes 3 and IVb and Figure S5a). Both structures **XX** and **XVIII** have a fairly expanded N−N bond length (1.36 Å). The energy of the intersection lies 73 kcal mol^{-1} above the ground-state minimum. The electronic structure of the T_1 and T_2 states in the vicinity of the intersection can be understood on the basis of the derivative coupling and gradient difference vectors (see ref 17a) of Figure S5a. In fact, the derivative coupling vector involves opening of the ∠NNC

Table 1. Ground and Excited State Energetics for the Potential Energy Surfaces of Diazabicyclo[2.2.1]hept-2-ene (DBH)

geometry	state	energy E_h CASSCF (6,5)	energy E_h MP2	rel energy, kcal mol^{-1} (zero pt energy corr)
DBH S_0 minimum	S_0	−302.9245[a]	−303.7680	0.0
(**A**, Figure S7a)	T_1 (n−π*)	−302.7980[b]	−303.6528	72.3
		−302.7511[c]		
	S_1 (n−π*)	−302.7702[b]	−303.6185	93.8
		−302.7212[c]		
	T_2 (π−π*)	−302.6962[c]		
DBH S_0 synchronous dissociation transition state (**XXIII**, Figure S7b)	S_0	−302.8750[a]	−303.7125	34.8 (29.8)
DBH S_0 C−N cleavage transition state (**IX**, Figure S2e)	S_0	−302.8491	−303.7196	30.4 (26.5)
S_0 endo diazenyl biradical minimum ($D'_{\sigma\sigma}$) (**VI**, Figure S2b)	S_0	−302.8503	−303.7212	29.4 (23.6)
S_0 exo−endo diazenyl biradical minimum ($D''_{\sigma\sigma}$) (**X**, Figure S2f)	S_0	−302.8497	−303.7205	29.8
S_0 exo diazenyl S_0 minimum ($D_{\sigma\sigma}$) (**IV**, Figure S2c)	S_0	−302.8525	−303.7225	28.6 (24.8)
S_0 diazenyl biradical dissociation transition state (**VIII**, Figure S2d)	S_0	−302.8697[†]	−303.7115	35.5 (29.9)
linear diazenyl biracial transition state (**II**, Figure S2a)	S_0	−302.8096	−303.6812	54.5
β C−C cleavage S_0 transition state (**XXXVI**, Figure S10a)	S_0	−302.8137[a]	−303.6568	69.8
DBH−azirane S_0 intermediate (**XXXII**, Figure S10b)	S_0	−302.7939	−303.6785	56.1
DBH−azirane S_0 transition state (**XXXIII**, Figure S10c)	S_0	−302.7938	−303.6782	56.3
azirane S_0 intermediate (**XXXIV**, Figure S10d)	S_0	−302.8497	−303.7627	3.3
azirane S_0 transition state (**XXXV**, Figure S10e)	S_0	−302.8475	−303.7593	5.5
azirane S_0 minimum (**D**, Figure S10f)	S_0	−302.8555	−303.7710	−1.9
DBH S_1 C_s transition state (**XIV**, Figure S4a)	S_1 (n−π*)	−302.7700[b]	−303.6207[b]	92.4
		−302.7245[c]		
DBH S_1 minimum (**XV**, Figure S4b)	S_1 (n−π*)	−302.7430	−303.6391	80.9 (79.5)
DBH S_1 transition state (**XVII**, Figure S4c)	S_1 (n−π*)	−302.7410	−303.6315	85.7
DBH S_1/T_2 crossing (**XVI**, Figure S4d)	S_1 (n−π*)	−302.7380	−303.6386	81.2
	T_2 (π−π*)	−302.7375	−303.6313	85.8
diazenyl S_0/S_1 conical intersection (**I**, Figure S1a)	S_0	−302.8043	−303.6764	57.5
	S_1 (n−π*)	−302.8039	−303.6759	57.8
DBH T_1 C_s transition state (**XXII**, Figure S6a)	T_1 (n−π*)	−302.7544[c]		
DBH T_1 skewed minimum (**XIX**, Figure S6b)	T_1	−302.7837[d]	−303.6904[d]	48.7
	T_2	−302.7040	−303.6006	106.0
DBH T_1 C_s transition state (**XXXVII**, Figure S6c)	T_1 (π−π*)	−302.7555[c]		
T_1 diazenyl biradical α C−N cleavage transition state (**XI**, Figure S6b)	T_1	−302.7729	−303.6648	64.8

Table 1 (Continued)

geometry	state	energy E_h CASSCF (6,5)	energy E_h MP2	rel energy, kcal mol^{-1} (zero pt energy corr)
T_1 endo diazenyl biradical minimum ($^3D'_{\sigma\sigma}$) (**VII**, Figure S3c)	T_1	−302.8500	−303.7203	29.9
T_1 endo−exo diazenyl biradical minimum ($^3D''_{\sigma\sigma}$) (**XII**, Figure S3d)	T_1	−302.8490	−303.7193	30.6
T_1 endo diazenyl biradical minimum (**V**, Figure S3e)	T_1	−302.8523	−303.7222	28.8
diazenyl biradical	S_0	−302.8525	−303.7225	28.6
S_0/T_1 crossing (**XIII**, Figure S3f)	T_1	−302.8522	−303.7223	28.7
linear diazenyl T_1 transition state (**III**, Figure S3a)	T_1	−302.8082	−303.6799	55.3
diazenyl T_1/T_2	T_1	−302.8035	−303.6756	58.0
conical intersection (**I**, Figure S1b)	T_2	−302.8033	−303.6753	58.2
β C−C cleave T_1 transition state (**XXIX**, Figure S9a)	T_1	−302.7487	−303.6525	72.5
DBH−azirane T_1 minimum (**XXX**, Figure S9b)	T_1	−302.7947	−303.6803	55.0
DBH−azirane S_0/T_1	T_1	−302.7943	−303.6766	57.3
crossing (**XXXI**, Figure S9c)	S_0	−302.7935	−303.6782	56.3
DBH T_2 minimum (**XX**, Figure S5b)	T_2	−302.7635[e]	−303.6551[e]	64.6
DBH T_2 transition state (**XXI**, Figure S5c)	T_2	−302.7474[f]		
DBH T_1/T_2 conical	T_1	−302.7558	−303.6524	72.5
itersection (**XVIII**, Figure S5a)	T_2	−302.7556	−303.6515	73.1

[a] 6 electron/6 orbital active space. [b] 8 electron/10 orbital acitive space. [c] 6 electron/4 orbital active space. [d] 4 electron/4 orbital active space. [e] State averaged orbitals used, forces only converged to 0.003. [f] State averaged orbitals used, forces only converged to 0.005.

and the gradient difference vector involves twisting of the C−N═N−C bridge. The ∠NNC distortion causes the "pure" (n−π*) and (π−π*) states to cross. Thus on one side of the upper (T_2) cone one has the (n−π*) **XX** and on the other side one has the (π−π*) structure **XVI** (this structure corresponds to a steep T_2/S_1 intersection point, and no stable (π−π*) minima has been located on T_2). The orthogonal C−N═N−C distortion has the effect of producing "mixed" (n−π*) and (π−π*) states, i.e., states which can be represented by a mixture of (n−π*) and (π−π*) character. Thus decaying from the tip of the conical intersection in the direction of the gradient difference vector generates the mixed (n−π*)−(π−π*) minimum **XIX** on the T_1 state (in this structure the n and π orbitals are strongly mixed so that the location of the two radical centers is not unambiguous). These effects are typical of the presence of a conical intersection: as one moves in a circle centered on the conical intersection point the wave function changes in a continuous fashion from (n−π*) to (n−π*)+(π−π*) to (π−π*) to (π−π*)−(n−π*) to −(n−π*). However, only the mixed (n−π*)−(π−π*) electronic structure generates a true minimum **XIX**.

One may ask why a twisted ^{1}(n−π*) structure does not exist. We have (in other unpublished work) optimized a twisted ^{1}(n−π*) for the parent (cyclic) compound pyrazoline (included as Supporting Information Figure S12a). In pyrazoline the ^{1}(n−π*) minimum has a 37° twist about the −N═N− bond consistent with the azomethane (liner) data. So there is a driving force for the twisting. On the other hand in the bicyclic compound 2,3-diazabicyclo [2.2.2] oct-2-ene (DBO included as Supporting Information Figure S12b) the twisting is very much reduced: only 1°. Since DBO is probably slightly less rigid than DBH, the explanation is that bicyclic compounds are sufficiently rigid to counterbalance the tendency to rotate. Thus one must conclude that the twisted ^{1}(n−π*) is unstable for steric reasons due to the fused rings. Further, the ^{3}(π−π*) state is a pure diradical as are the ^{1}(n−π*) and ^{3}(n−π*) states. However, the pure ^{1}(π−π*) state is an ionic/Rydberg (like the V state in ethylene). Thus while the ^{3}(n−π*) can mix ^{3}(π−π*) to stabilize a twisted intermediate, the ^{1}(n−π*) and ^{1}(π−π*) will not mix substantially.

As described in Scheme 3, a T_2 (π−π*) molecule, prepared either by ISC after direct irradiation (see above) or by sensitized irradiation, can evolve via two possible routes. The first route involves decay through the T_1/T_2 conical intersection described above, and subsequent relaxation to a triplet intermediate **XIX** lying 24 kcal mol^{-1} below the T_1/T_2 conical intersection **XVIII**. As shown in Scheme 3 we have located a C−N ring-opening transition state (**XI**, Figure S3b) 16 kcal mol^{-1} above the twisted minimum **XIX**, as described earlier. A MEP computation from this transition state leads to a $^3D_{\sigma\sigma}$ intermediate (structure **VII**, Figure S3c) in one direction and the minimum **XIX** in the other. Therefore, if the T_1 state is populated, a dissociative $^3D_{\sigma\sigma}$ diazenyl biradical (**V**) can be formed via the C−N bond cleavage over a barrier of 16 kcal mol^{-1} followed by the twisting of the N−N moiety around the C−N bond. As will be shown in subsection (**iii**), the rotation of the N−N moiety around this C−N bond in the T_1 state has almost no barriers.

Scheme 3

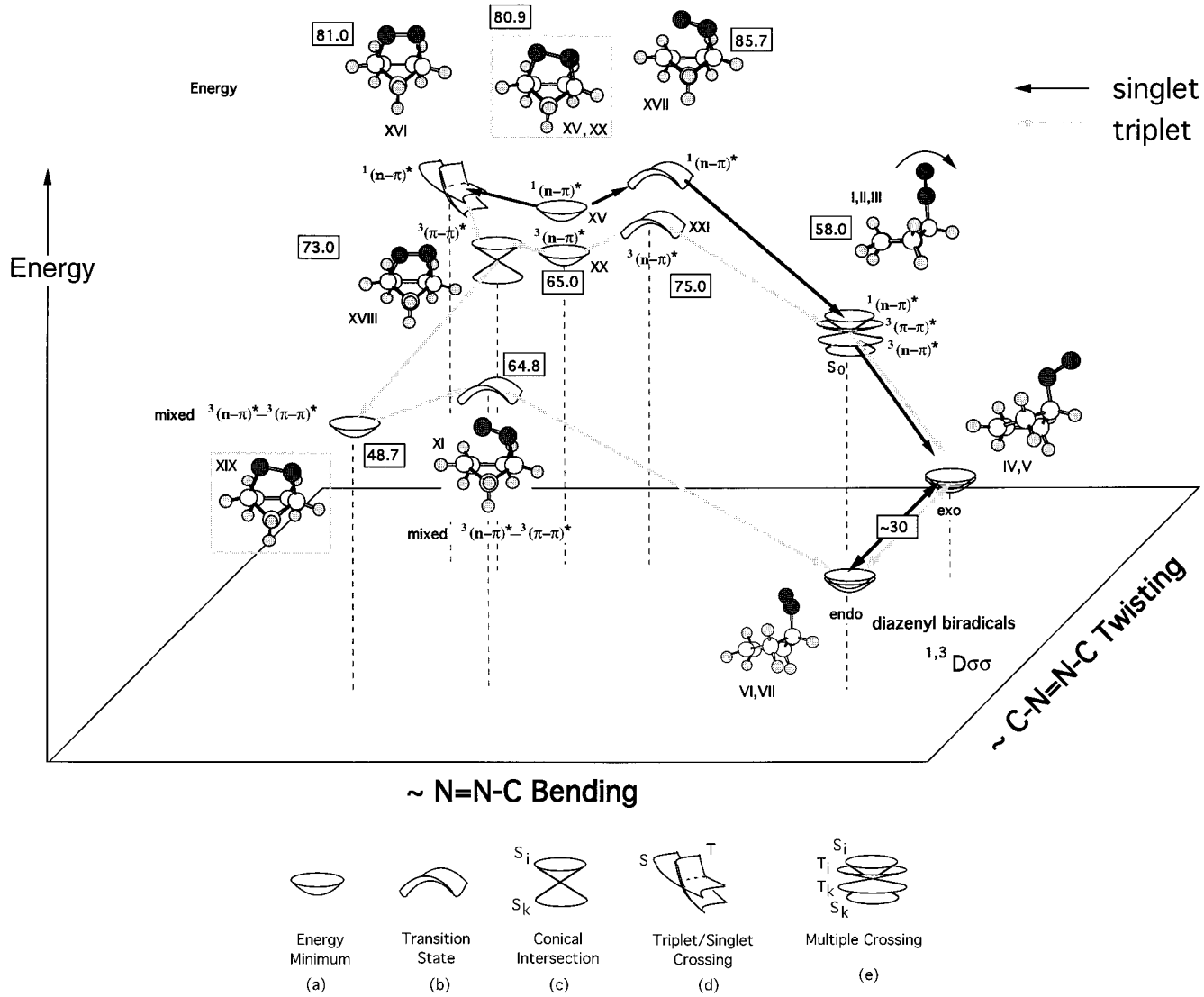

A second possible route for the evolution of T_2 ($\pi-\pi^*$) DBH involves population of a T_2 excited state $^3(n-\pi^*)$ minimum located in the vicinity of the T_1/T_2 conical intersection ca. 8 kcal mol^{-1} below the T_1/T_2 structure and at a more expanded N−N bond length (N−N = 1.40 Å). About 10 kcal mol^{-1} above this minimum, we find a C−N ring-opening transition state (structure **XXI**, Figure S5c), which leads to the same 4-fold crossing point (structure **I**) discussed above. As in the case of the S_1 transition structure **XVII**, this crossing provides a very efficient decay pathway to the exo $^3D_{\sigma\sigma}$ diazenyl biradical. Hence direct nitrogen extrusion is also possible via triplet sensitized to the T_2 state, relaxation to the $^3(n-\pi^*)$ minimum **XX**, and ring-opening through the transition state **XXI**. Alternatively, it is also conceivable (see Scheme 3) that from the minimum **XX** the system could evolve back toward the T_1/T_2 conical intersection and produce the triplet intermediate **XIX** via $T_1 \rightarrow T_2$ decay.

To complete our discussion of the triplet potential energy surfaces of DBH, let us now consider the structure of the T_1 ($n-\pi^*$) state in the Franck−Condon region. This is illustrated in Scheme 4b. Like the S_1 ($n-\pi^*$) state, we have located a transition state near the Franck−Condon region (structure **XXII**, Figure S6a). The structure of this transition state has C_s symmetry. However, the normal coordinate corresponding to the imaginary frequency (577i cm^{-1}) involves C−N═N−C bridge twisting in contrast to ∠CNN opening for the S_1 ($n-\pi^*$) state. By following the transition vector, we reach two equivalent T_1 minima **XIX**. This transition state is connected to the higher T_1/T_2 conical intersection seen above (structure **XVIII** in Schemes 3 and 4b) via a −N═N− stretching expansion motion (−N═N− goes from 1.26 to 1.36 Å). We have optimized another T_1 transition state (**XXXVII**, Figure S6c) with C_s symmetry at a longer N−N distance (N−N = 1.50 Å). While the first C_s transition state belongs to the $^3(n-\pi^*)$ state, this C_s transition state has $^3(\pi-\pi^*)$ character. The transition vector also corresponds to C−N═N−C bridge twisting and connects the same two equivalent T_1 skewed minima (**XIX**). Thus, as one goes around in a "circle" about the T_1/T_2 conical intersection, one encounters a $^3(\pi-\pi^*)$ transition state (**XXXVII**) and a $^3(n-\pi^*)$ transition state (**XXII**) as well as the equivalent T_1 minima **XIX**. Notice that the $^3(\pi-\pi^*)$ transition state (**XXXVII**) and a $^3(n-\pi^*)$ transition state (**XXII**) lie on the "lower sheet" of the conical intersection (i.e. T_1); accordingly they must lie below the intersection and the $^3(n-\pi^*)$ minimum, which occurs on the upper sheet (T_2). These structures lie so close to the intersection that they could only be optimized with a reduced active space, so the energies in Table 1 are not comparable with those of the other structures, thus the energetics of these structures (shown in Scheme 4b) are estimates.

At this stage, we can comment on the nature of the triplet

Scheme 4

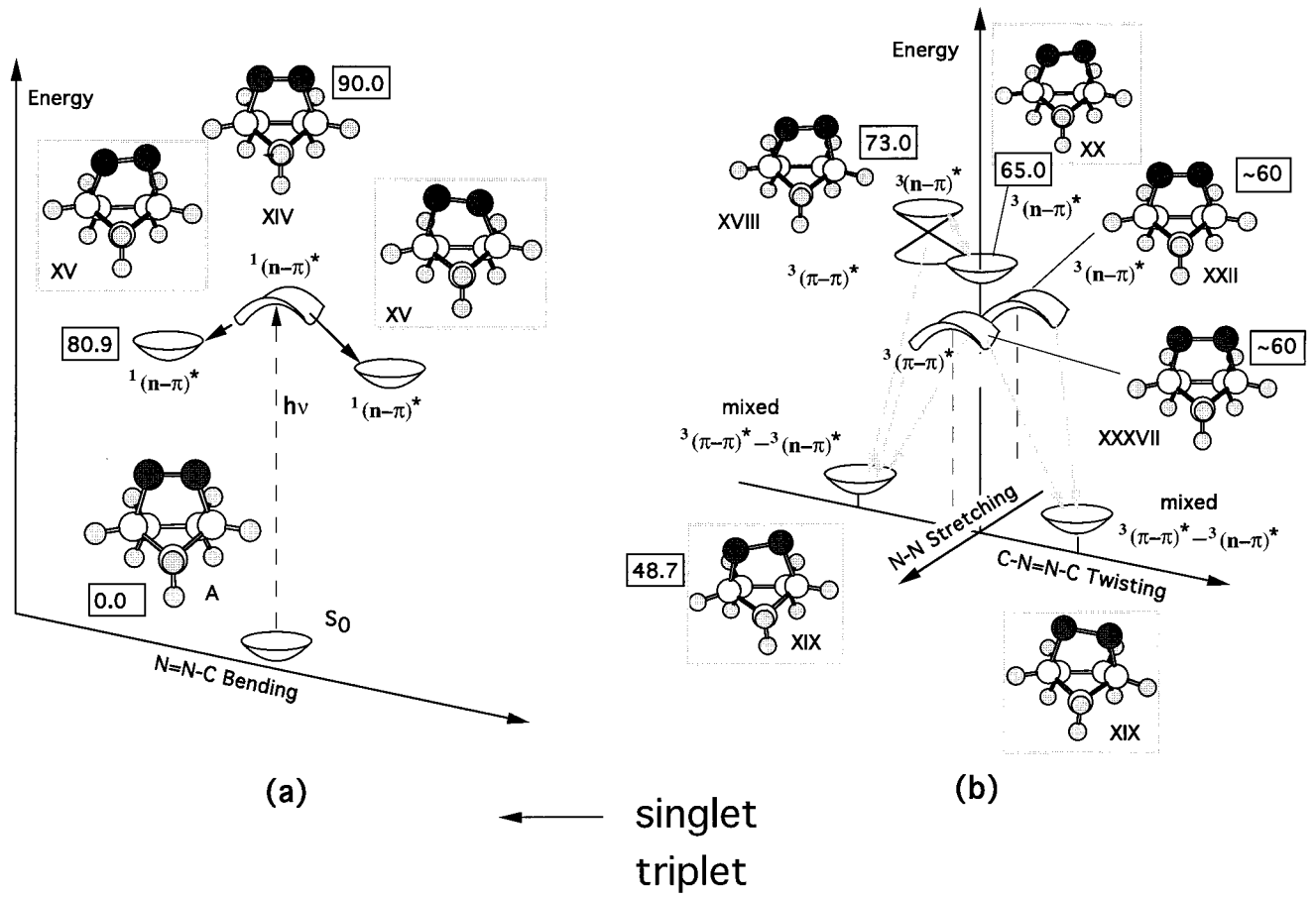

metastable species with a lifetime of 25 ns, which has been detected during direct photolysis of DBH in the gas phase.[8] Clearly, this species will be reached after efficient ISC from the S_1 ($n-\pi^*$) to the T_2 ($\pi-\pi^*$) state via S_1/T_2 crossing (structure **XVI** in Scheme 3). As the N−N bond is stretched from this S_1/T_2 crossing region (N−N bond length = 1.32 Å), the $^3(n-\pi^*)$ and $^3(\pi-\pi^*)$ states cross at a T_1/T_2 conical intersection where the N−N bond length is 1.36 Å (structure **XVIII**, Figure S5a). This conical intersection provides a funnel for a decay from the T_2 to T_1 surface leading to the twisted minimum **XIX**. We have found that there is a barrier of ca. 16 kcal mol^{-1} from the T_1 minimum (transition state structure **XI**) to the endo diazenyl biradical ($^3D'_{\sigma\sigma}$, **VII**). It has been observed that in the gas-phase photolysis ($\lambda = 338$ nm (84.5 kcal mol^{-1})) the decay lifetime of the S_1 state is 2 ns while the appearance time of free N_2 is 25 ns.[8] This suggests that when the reactant is excited in the vapor phase with irradiation wavelength just below the S_1 ($n-\pi^*$) C−N ring-opening transition state (**XVII**), it will undergo efficient ISC (corresponding to $\tau = 2$ ns) to the T_2 ($\pi-\pi^*$) state. This will be followed by efficient IC to the T_1 intermediate (structure **XIX**) via T_1/T_2 conical intersection (structure **XVIII**). As we will see in subsection (**iii**), we expect the lifetime of the diazenyl biradical to be very short because there is no barrier for dissociation in the triplet diazenyl biradical region and, in general, lifetimes of open-chain biradicals are known to be short (<20 ns).[25] Therefore, *we assign the metastable species* ($\tau \sim 25$ ns) to the T_1 minimum (**XIX**). Our conclusion is also supported by the fact that there have been at least two cases for which triplet quenchers affected the product distribution obtained on direct irradiation of some DBH derivatives.[26]

Further evidence in favor of the assignment of a relatively long-lived triplet intermediate to structure **XIX** comes from the experiments on substituted DBH. (A long-lived azoalkane triplet state has been identified in the direct photolysis of the DBH derivative **A′**. This long-lived intermediate ($\tau \sim 630$ ns) is also assigned to the same T_1 intermediate.) Adam et al. has confirmed the existence of the metastable triplet state in fused DBH derivatives[4c] which lies 62.5 ± 1 kcal mol^{-1} above the reactant minimum. Our CAS/MP2 calculation on the parent compound places this minimum about 10 kcal mol^{-1} lower in energy. Adam and co-workers have also observed the T−T absorption band of the DBH derivative in the UV region (1.8 eV = 41.5 kcal mol^{-1}).[4c] Our computed T_1-T_2 energy difference at the parent compound T_1 minimum (**XIX**) is 56 kcal mol^{-1}, which is close to the experimental result (considering that our T_1 minimum energy differs by 10 kcal mol^{-1}). The activation energy for the C−N α cleavage from the triplet state of the fused derivative of DBH (structure **A′** in Scheme 1) is known to be ≥10.5 kcal mol^{-1},[4b,c] so our computed (16 kcal mol^{-1}) barrier height falls, again, in the same energy range.

(ii) Direct and Sensitized Photochemical Production of Hydrazonyl Biradical Intermediates ($^{1,3}D_{\sigma\pi}$). Recently, Adam and co-workers[4a−c] observed that in direct and triplet-sensitized photolysis, some DBH derivatives do not only give the expected housane (structure **E**) through a C−N cleavage and subsequent

(25) Johnston, L.; Scaiano, J. C. *Chem. Rev.* **1989**, *89*, 521.

(26) (a) Adam, W.; Hill, K. *J. Am. Chem. Soc.* **1985**, *107*, 3686. (b) Adam, W.; Grabowski, S.; Platsch, H.; Hannemann, K.; Wilson, R. M.; Wirtz, J. *J. Am. Chem. Soc.* **1989**, *111*, 751.

Scheme 5

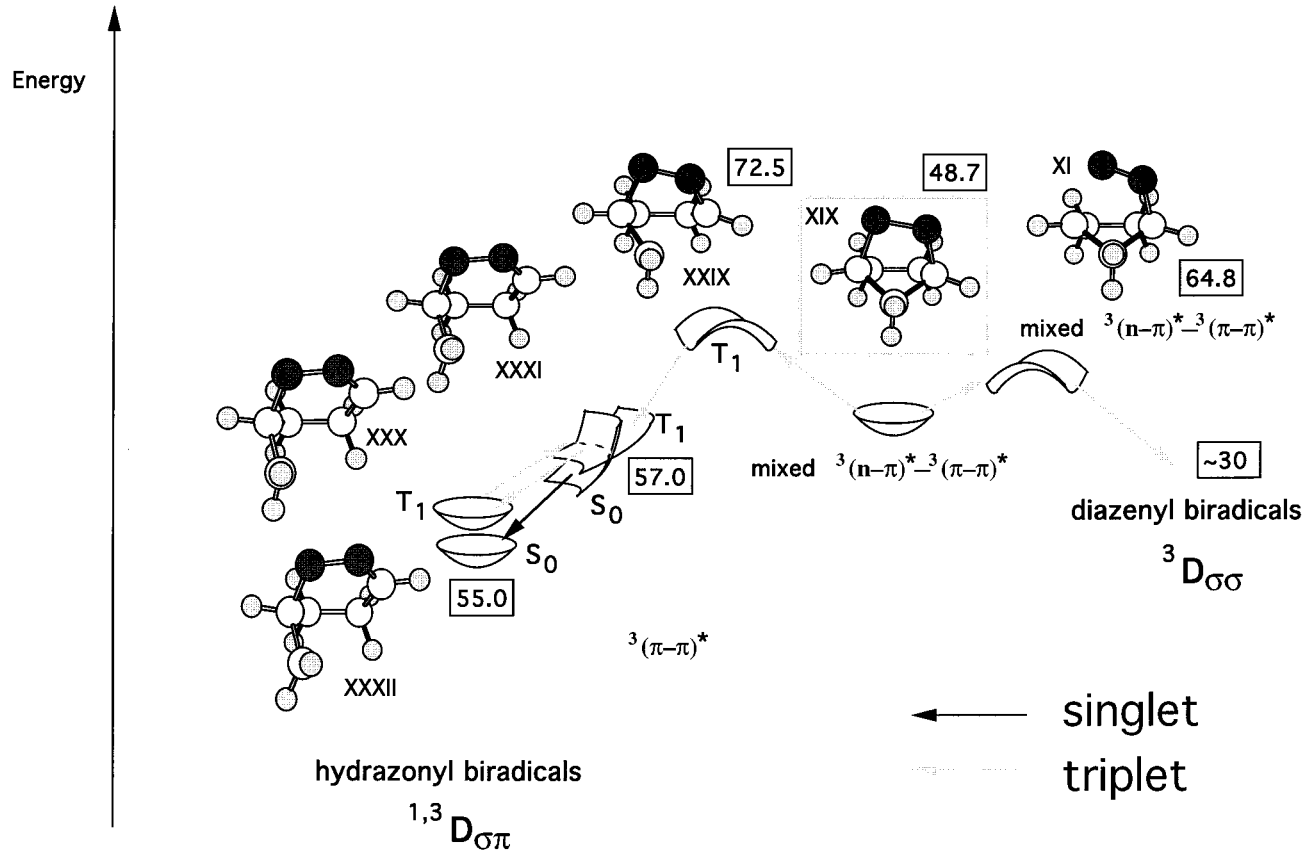

Scheme 6

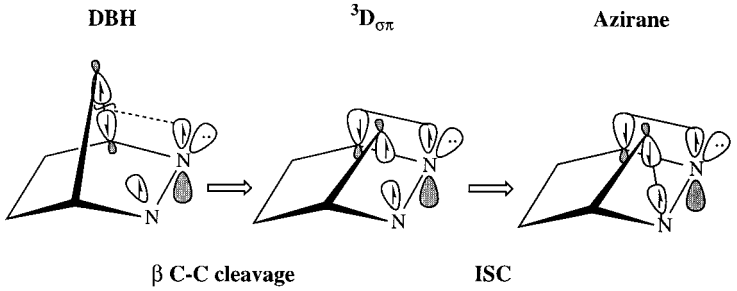

denitrogenation but also yield the rearrangement product azirane through β C−C cleavage (structure **J′** in Scheme 1). Their results indicate that the housane (structure **E**)/azirane (structure **J′**) ratios of the direct and triplet-sensitized photolysis are strongly temperature dependent; in both cases the housane increased at higher temperature. Although β C−C scission is only observed in photolysis of fused derivatives of DBH (e.g. *anti*-hexahydro-1,4:5,8-dimethanophthalazines, shown as structure **A′**), we have located and studied the β C−C cleavage reaction paths in unsubstituted DBH. (Note that Adam and coworkers have also observed β C−C cleavage from the diazenyl radicals[4e] to give diazoalkanes derived from other systems, but we have not explored this possibility for DBH.) A schematic representation of the β C−C scission reaction pathway is shown in Scheme 5.

The β C−C bond cleavage is observed in both direct and triplet-sensitized photolysis but it is thought to take place in the triplet state.[4] Accordingly, we have searched for a C−C cleavage transition state on the T_1 state (the alternative, β C−C cleavage on the S_1 state, has not been investigated in this paper) and successfully located this transition state (structure **XXIX** in Scheme 5) at an energy 24 kcal mol^{-1} above the skewed T_1 minimum (structure **XIX**, Figure S6b). The structure of the transition state is shown in Figure S9a together with its transition vectors. A MEP computation from this transition state (**XXIX**) leads back to the skewed minimum (**XIX**) in one direction and to a hydrazonyl biradical ($^3D_{\sigma\pi}$) (structure **XXX,** Figure S9b, shown as **G′** in Scheme 1) in the other. The electronic structure of this biradical intermediate is shown in Scheme 6.

To form azirane (**J**) from the triplet hydrazonyl biradical, the molecule must undergo ISC to the S_0 state. We have also found an S_0/T_1 crossing (structure **XXXI**, Figure S9c) near the $^3D_{\sigma\pi}$ biradical. The SOC between S_0 and T_1 is negligible (<1 cm^{-1}) since $^3D_{\sigma\pi}$ and $^1D_{\sigma\pi}$ are perfect biradicals. However, the existence of the T_1 minimum (**XXX**) in the vicinity of the crossing should increase the probability of ISC because the molecule can oscillate in the region of the minimum many times, losing some of its kinetic energy until it is moving sufficiently slowly to pass through the crossing onto the ground-state surface. Also, the gradient difference is found to be very small (0.0056 hartree/Bohr) at this crossing (**XXXI**). Therefore the molecule will be able to undergo ISC eventually. Once the molecule gets into the ground state, it will decay toward a singlet

$^1D_{\sigma\pi}$ hydrazonyl biradical (**XXXII**, Figure S10b, shown as **G′** in Scheme 1) which is located very close to the S_0/T_1 crossing (**XXXI**).

As already illustrated in Scheme 3, in the direct photolysis, the excited molecule can efficiently decay from the S_1 state to the T_1 state via S_1/T_2 crossing (structure **XVI** in Scheme 3) followed by IC via T_1/T_2 conical intersection (structure **XVIII**). As reported in Scheme 5 this intermediate can give either β C−C ring-opening leading to hydrazonyl biradicals or α C−N ring-opening leading to diazenyl biradicals.

So far, we have established that there exist β C−C scission reaction paths for unsubstituted DBH. However, the energy of the β C−C ring-opening transition state (structure **XXIX** in Scheme 5) is ca. 8 kcal mol^{-1} higher than that for the α C−N ring-opening transition state (**XI**), which explains why the β C−C cleavage reaction has not been observed in unsubstituted DBH but only in DBH derivatives with a bridging substituent (e.g. **A′** in Scheme 1). To estimate the effect of the bridging substituent, we re-optimized (crudely at the UHF/STO-3G level) the T_1 skewed minimum (**XIX**, Figure S6b) from which the β C−C breakage takes place with a bridging substituent. In Figure S11, we have shown the optimized structures of T_1 minimum for unsubstituted (Figure S11a) and substituted (Figure S11b) DBH. The UHF geometry for the unsubstituted DBH (Figure S11a) is in good agreement with the MC-SCF structure (Figure S6b). One can see that increasing molecular rigidity decreases the ∠CNNC dihedral angle from 17° to 0.2°, i.e., reduces "twisting" about the C−N═N−C bridge. Thus, there appears to be a structure/reactivity correlation, and one may expect that the activation energy for the β C−C cleavage will be lowered for DBH derivatives with some bridging substituent. Therefore, the β C−C ring-opening reaction will be able to compete with α C−N ring-opening in DBH derivatives such as *anti*-hexahydro-1,4:5,8-dimethanophthalanzines (**A′** in Scheme 1).

The observed strong temperature dependence in the β C−C/α C−N yield ratio from DBH derivatives must be related to the ratio of the corresponding barriers from the long-lived T_1 intermediate **XIX** (see Scheme 5). Low temperature must favor the less energy demanding process (i.e., presumably, the β C−C in DBH derivatives).

(iii) The Structure and Fate of Diazenyl and Hydrazonyl Biradicals. The purpose of this subsection is to discuss the structure of the diazenyl and hydrazonyl biradical region of the T_1 and S_0 potential energy surface.

(a) Diazenyl Biradicals ($^{1,3}D_{\sigma\sigma}$). As illustrated in Figure 3, the diazenyl biradical exists in a C−N−N "bent" ($D_{\sigma\sigma}$, $D'_{\sigma\sigma}$, and $D''_{\sigma\sigma}$) form or in a C−N−N "linear" form. The bent form corresponds to a real biradical intermediate with three possible conformations (exo, endo, or endo−exo). As described above the linear form corresponding to structure **I** (Scheme 3) corresponds to an *highly unstable* configuration where the S_0, $^3(\pi-\pi^*)$, $^3(n-\pi^*)$, and $^1(n-\pi^*)$ states are degenerate and forms a multiple funnel. Linear forms (for the S_0 and $^3(n-\pi^*)$ states) of diazenyl biradical also exist as high energy S_0 and T_1 transition states (structures **II** (Figure S2a) and **III** (Figure S3a) respectively) for inversion between exo (**IV** (Figure S2c), **V** (Figure S3e)) and endo (**VI** (Figure S2b), **VII** (Figure S3c)) forms. The endo, exo, and endo−exo (**X** (Figure S2f), **XII** (Figure S3d)) forms are interconverted via rotation of the N−N moiety around the C−N bond. However, *the barriers are so low that we could not determine these transition states accurately*.

As illustrated in Scheme 7a, the potential energy surface of the S_0 bent diazenyl biradical is *extremely* flat (the lowest positive vibrational frequencies of the endo and exo forms are less than 100 cm^{-1}) and the computed barriers for fragmentation and ring-closure are also negligible (being comprised in a range of a few kilocalories per mole). Thus, the S_0 diazenyl biradical is actually a *transient* species with a short lifetime. Similarly,

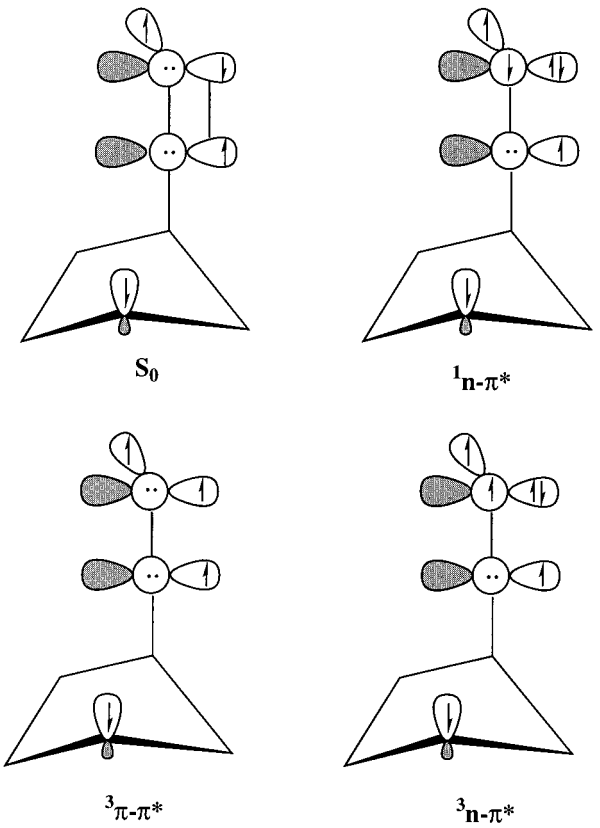

Figure 2. Electronic structures at the 4-fold crossing point.

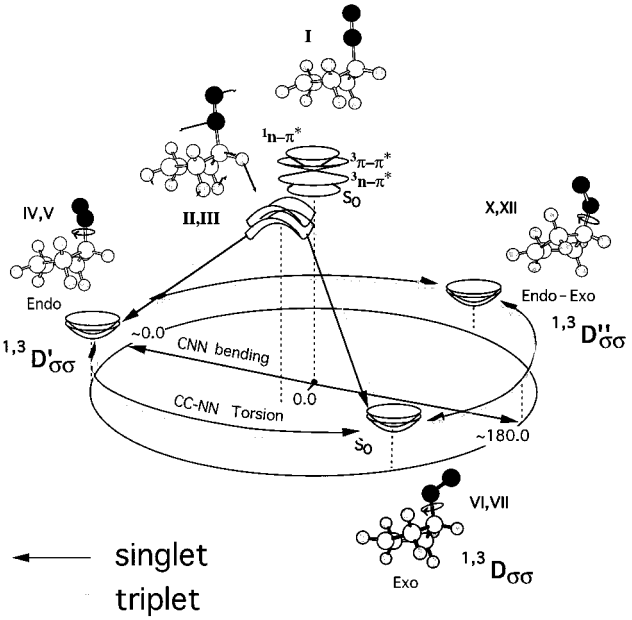

Figure 3. A schematic polar (r,θ) representation of the structure of the S_0 potential energy surface around the 4-fold crossing point. (r = CNN bending, θ = CC−NN torsion). The stationary points are as follows: (a) the 4-fold crossing (**I**), (b) linear singlet and triplet transition states (**II**, **III** respectively), (c) singlet diazenyl biradical minima—exo ($^1D_{\sigma\sigma}$) (**VI**), endo ($^1D'_{\sigma\sigma}$) (**IV**), and exo−endo ($^1D''_{\sigma\sigma}$) (**X**), and (d) triplet diazenyl biradical minima—exo ($^3D_{\sigma\sigma}$) (**VII**), endo ($^3D'_{\sigma\sigma}$) (**V**), and exo−endo ($^3D''_{\sigma\sigma}$) (**XII**).

Scheme 7

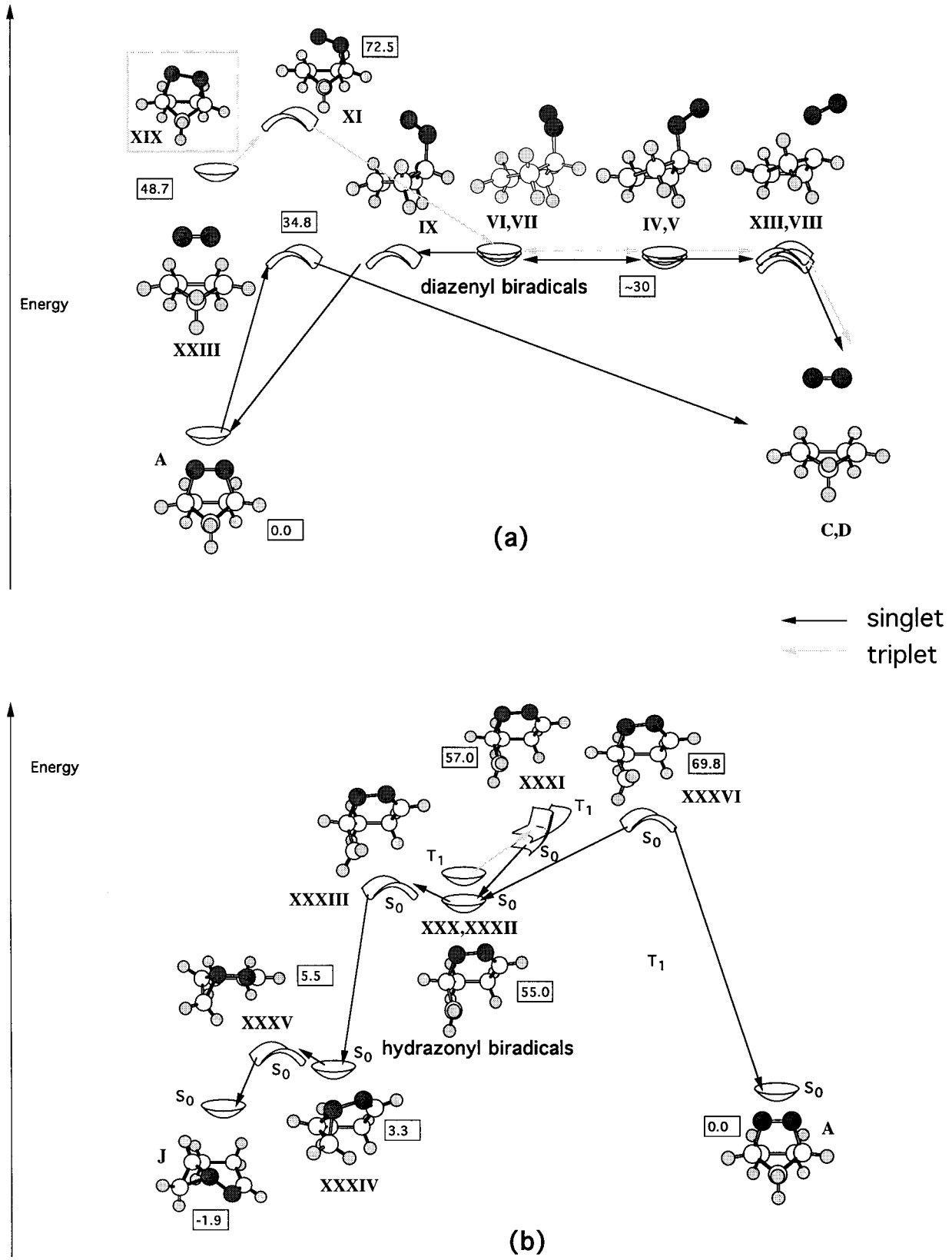

the region of the T_1 potential energy surface corresponding to the bent diazenyl biradical minima is extremely flat, and we could not optimize the transition states connecting the endo−exo biradical minimum $^3D''_{\sigma\sigma}$ (**XII**) to the other bent triplet biradical minima $^3D_{\sigma\sigma}$ and $^3D'_{\sigma\sigma}$ (**VII**, **V**). However, the energy of the ring-closure transition state (**XI**, Figure S3b) connecting the bent biradical minima to the mixed $^3(n-\pi^*)-^3(\pi-\pi^*)$ intermediate (**XIX**) is much higher than in S_0 ring-closure (via transition state **IX,** Figure S2e) where reactant back-formation is substantially barrierless. In contrast, no barrier has been found for fragmentation (with N_2 extrusion) from the exo $^3D_{\sigma\sigma}$ diradical (**V**). Notice that the transition structure **IX** is also involved in the ground state (thermal) generation of endo diazenyl biradicals. The associated thermal α C−N cleavage barrier is found to be

about 30 kcal mol^{-1}. We have found that this ground-state barrier is of the same magnitude of the barrier found along the concerted pathway corresponding to the transition structure **XXIII** (Figure S7b). Thus our computations suggest that nitrogen loss via concerted synchronous and asynchronous paths is nearly competitive. More accurate computations are required for solving the delicate quantitative problem of the competition between these two paths in DBH.

The linear diazenyl biradical region of the potential energy surface deserves a more detailed description. At structure **I** in Figure 3 the S_0, $^3(\pi-\pi^*)$, $^3(n-\pi^*)$, and $^1(n-\pi^*)$ states become degenerate so that conversion between all of these states is (in principle) possible. The origin of the 4-fold crossing can easily be rationalized from the character of the two unpaired electrons in these structures (see Figure 2). These two electrons can be considered almost uncoupled from each other, and since the coupling between the two radical centers is so small, the triplet and singlet states must be degenerate. Furthermore, at the nitrogen atom, one is left with a singly occupied p-orbital and a lone-pair located along orthogonal axes in space. The $^1(n-\pi^*)$ and $^3(n-\pi^*)$ states can be derived from the S_0 and $^3(\pi-\pi^*)$ states by swapping the relative occupancies of the singly occupied p-orbital and lone-pair. However, this difference will not affect the energy and therefore all four states ($^1(n-\pi^*)$, S_0, $^3(n-\pi^*)$, and $^3(\pi-\pi^*)$) will be degenerate. This behavior is consistent with the directions defined by the gradient difference and derivative coupling vectors at the multiple funnel (corresponding to "superimposed" S_0/S_1 and T_1/T_2 conical intersections (Figure S1)) which indicate the type of molecular distortion required to lift the degeneracy. These vectors correspond to two "orthogonal" bendings of the ∠NNC angle, which would split the degeneracy by increasing the coupling between the two radical centers. The SOC computed between singlet and triplet surfaces with different electronic configurations (i.e. $^1(n-\pi^*)/^3(\pi-\pi^*)$ and $^3(n-\pi^*)/S_0$) was found to be large (15.2 and 15.2 cm^{-1} respectively), but small (<1 cm^{-1}) between surfaces with the same electronic configurations. Since the velocity of the decaying system near structure I must be high, a low efficiency is predicted for ISC in this region.

The fate (see Scheme 7a) of the system immediately after conversion at the 4-fold degeneracy will be controlled, in part, by the shape of the S_0 and T_1 surfaces in the immediate vicinity of the multiple funnel (**I**, Figure 3). Using a geometry optimization method designed to probe the region of surface crossings,[27] we have found a new stationary point on the S_0 surface in the vicinity of the degeneracy corresponding to a linear transition state **II** at 54.5 kcal mol^{-1} above the reactant minimum (**A**). The transition vector corresponding to the imaginary frequency (1051*i* cm^{-1}) of the transition state **II** involves the ∠NNC bend. A MEP computation from this transition state leads to the endo biradical minimum $^1D'_{\sigma\sigma}$ in one direction and the exo biradical minimum $^1D_{\sigma\sigma}$ (**IV**) in the other direction. We have found that the nitrogen extrusion occurs from this exo diazenyl biradical over a loose transition structure (**VIII**, Figure S2d) with a 7 kcal mol^{-1} barrier. The bent α C−N ring-opening transition state **IX** connects the endo biradical minimum $^1D'_{\sigma\sigma}$ to the reactant minimum (**A**) via a CC−NN torsion corresponding to a barrier of 1 kcal mol^{-1} for the ring closure. Our CAS/MP2 calculations reveal that all bent biradicals (the C−N ring-opening transition state (**IX**), endo $^1D'_{\sigma\sigma}$ (**VI**), endo−exo $^1D''_{\sigma\sigma}$ (**X**), and exo $^1D_{\sigma\sigma}$ (**IV**) biradical minima) lie between 28 and 31 kcal mol^{-1} relative to the reactant minimum (**A**). The computed imaginary frequency for the transition state **IX** is 137*i* cm^{-1} and the lowest positive frequencies of the exo $^1D_{\sigma\sigma}$, endo−exo $^1D''_{\sigma\sigma}$, and endo $^1D'_{\sigma\sigma}$ biradical minima are all around 75−90 cm^{-1}. Thus, the region of bent diazenyl biradical surface is very flat, i.e., the N_2 moiety can rotate around the C−N bond almost freely. The flat nature of the bent biradical potential energy surface also explains why we could not locate any transition states connecting the endo−exo $^1D''_{\sigma\sigma}$ biradical (**X**) to the endo $^1D'_{\sigma\sigma}$ (**VI**) or to the exo $^1D_{\sigma\sigma}$ (**IV**) biradical minimum.

We have found similar features on the T_1 surface around the 4-fold crossing (**I**): a linear transition state adjacent to the 4-fold crossing (**III**, Figure S3a), a bent C−N ring-opening biradical transition state (**XI**), and bent diazenyl biradical minima (endo $^3D'_{\sigma\sigma}$ (**VII**), endo−exo $^3D''_{\sigma\sigma}$ (**XII**), and exo $^3D_{\sigma\sigma}$ (**V**)). The linear transition state (**III**) connects the endo (**VII**) and exo (**V**) biradicals whereas the C−N ring-opening biradical transition state (**XI**) links the endo biradical minimum to the T_1 DBH minimum (**XIX**). However, the energy of the triplet C−N ring-opening transition state **XI** relative to the bent biradical minima (endo $^3D'_{\sigma\sigma}$ (**VII**), endo−exo $^3D''_{\sigma\sigma}$ (**XII**), and exo $^3D_{\sigma\sigma}$ (**V**)) is much higher than in the singlet case. Also, no barrier has been found for the N_2 extrusion from the exo $^3D_{\sigma\sigma}$ diradical (**V**).

It must be noted that the S_0 and T_1 surfaces are found to be degenerate everywhere along the reaction coordinate connecting the four-surface crossing point (**I**) and the exo diazenyl biradical minima ($^1D_{\sigma\sigma}$ (**IV**) and $^3D_{\sigma\sigma}$ (**V**)). In fact, the lowest energy point on this crossing seam has been located very close to these exo biradical minima (compare structures **IV**, **V**, and **XIII**, Figure S3f). However, the computed value of the SOC at this crossing is negligible (<1 cm^{-1}). This can be rationalized by the fact that the S_0 and T_1 states are perfect $\sigma\sigma$ biradicals. Thus, we expect ISC between the singlet and triplet exo diazenyl biradicals ($^1D_{\sigma\sigma}$ (**IV**) and $^3D_{\sigma\sigma}$ (**V**)) to be relatively inefficient since the spin-flip between two perfect biradicals does not induce a large change in orbital angular momentum. Therefore, whether the fragmentation takes place in the T_1 or S_0 state depends on which electronic state is initially populated and how the excited molecule enters this diazenyl biradical region (shown as **B** in Scheme 1).

(b) Hydrazonyl Biradicals ($^{1,3}D_{\sigma\pi}$). As seen above, β C−C cleavage can take place on the T_1 surface due to the incipient allylic stabilization of the resulting hydrazonyl biradical. This explains why azirane becomes a dominant product in the triplet-sensitized photolysis of some DBH derivatives. However, the formation of azirane depends partly on the efficiency of ISC after the β C−C bond breakage. This is achieved via the singlet triplet crossing **XXXI** and results in formation of the singlet hydrazonyl biradical **XXXII**. However, the fact that the yield of azirane is strongly temperature dependent must be mainly associated with the different activation energies of α and β cleavage. The fate of the hydrazonyl biradical generated via conversion of the excited-state triplet intermediate **XXX** is illustrated in Scheme 7b. The singlet biradical generates a bicyclic intermediate (structure **XXXIV**, Figure S10d) by passing over a very small barrier (**XXXIII**, Figure S10c). Finally, the azirane S_0 minimum (**J**, Figure S10f) is reached via another transition state (**XXXV**, Figure S10e) 2 kcal mol^{-1} above this intermediate (**XXXIV**). It should be noted that the direct β-cleavage path on the ground state involves a transition state (**XXXVI**, Figure s10a) which is located some 70 kcal mol^{-1} above the reactant minimum (**A**). This is consistent with the fact that the β-scission reaction can only be observed during photolysis, but not in thermolysis.

(27) Celani, P.; Robb, M. A.; Garavelli, M.; Bernardi, F.; Olivucci, M. *Chem. Phys. Lett.* **1995**, *243*, 1.

Scheme 8

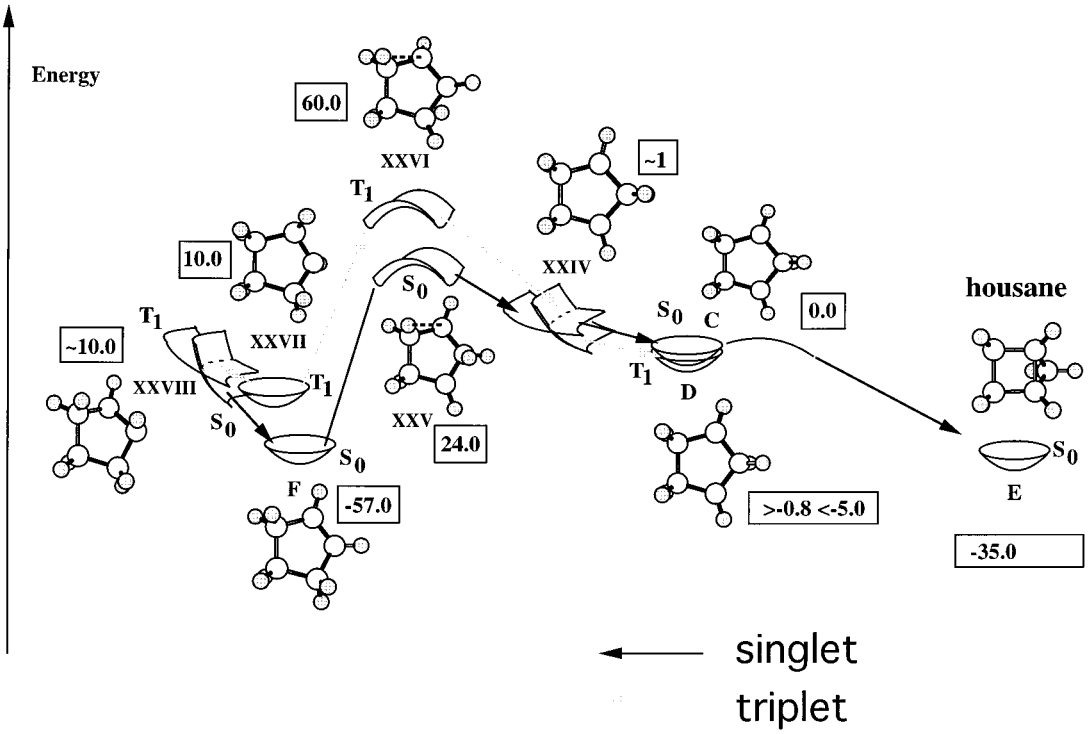

(iv) Cyclization versus Rearrangement of 1,3-Cyclopentanediyl Diradical. Once the 1,3-diradical (shown as **C** and **D** in Scheme 1) has been generated via denitrogenation, its chemical fate with respect to cyclization into housane (**E**) vs rearrangement to cyclopentene (**F**) has been of considerable mechanistic interest.[28] The long-standing puzzle has been the fact that the triplet-sensitized denitrogenation of DBH gave predominantly, if not exclusively, cyclization while the direct photolysis led at least to some rearrangement. There has been an ab initio study on singlet and triplet 1,3-cyclopentanediyl (**C**, **D**) and housane (**E**) using a DZ+d basis set at the SCF and CISD levels of theory by Schaefer et al. In this work, we have characterized the reaction pathways from triplet and singlet 1,3-cyclopentanediyl biradicals (**C**, **D**) to both housane (**E**) and cyclopentene (**F**) using the MC-SCF method with the 6-31G* basis.

A schematic representation of S_0 and T_1 potential energy surfaces associated with 1,3-cyclopentanediyl rearrangement/cyclization is shown in Scheme 8 (energies relative to the S_0 1,3-cyclopentanediyl biradical **C**). Energetics are collected in Table 2. Our results indicate that there is a shallow minimum on the singlet 1,3-cyclopentanediyl surface (the lowest positive frequency is 117 cm^{-1}), in accord with the result obtained by Schaefer et al. The structures of T_1 and S_0 1,3-cyclopentanediyl minimum are very similar (**C**, Figure S8a and **D**, Figure S8b). The energy of the T_1 minimum (**D**) lies slightly lower (0.8 kcal mol^{-1}) than that of S_0 (**C**) at the CAS-SCF level and 4.9 kcal mol^{-1} lower at the MP2 level of theory. (Schaefer et al.[16a] find an energy difference of 0.8 kcal mol^{-1} at the CAS level and 1.10 kcal mol^{-1} when the geometries are re-optimized including dynamic correlation. The discrepancy between our CAS MP2 results and the results of Schaefer when dynamic correlation is included stems from two factors: (a) effects of geometry optimization including dynamic correlation and (b) a slight difference between the reference Hamiltonian used in ROMP2 (used for D) and the CAS MP2 method (used for C)) since 2 electron triplet **D** is computed as a single configuration a ROHF/ROMP2 problem. We have located (also with two active orbital CAS) a S_0/T_1 crossing (**XXIV**, Figure S8c) very close to these minima. The computed SOC constant at this crossing is negligible (<1 cm^{-1}). This is to be expected since the S_0 and T_1 are perfect biradicals, hence the spin flip does not induce a large orbital angular momentum change. However, the gradient difference is found to be small (0.0068 hartree/Bohr). Therefore, ISC to S_0 will take place eventually. Our results show that cyclization of singlet 1,3-cyclopentanediyl to form housane (**E**, Figure S8d) occurs with virtually no barrier, while Schaefer's results indicate that there is a barrier of *less than 1* kcal mol^{-1} above the singlet 1,3-biradical minimum. Therefore, if the 1,3-biradical is formed as a singlet, it would almost certainly form housane by rapid ring closure. On the other hand, if 1,3-cyclopentanediyl is created as a triplet, the cyclization to housane would be delayed by the need for spin change, which would be very slow due to the small spin−orbit coupling. Since the lifetime of a precursor of the photofragments is known to be a few hundred nanoseconds,[2,8,10b,13,15] it can be concluded that the gas-phase photochemical nitrogen extrusion occurs predominantly on the triplet surface.

We have also searched for a hydrogen shift transition state of the 1,3-cyclopentanediyl on both triplet and singlet surfaces (**XXV**, Figure S8e and **XXVI**, Figure S8f). The energy of the S_0 H-shift transition state (**XXV**) lies 25 kcal mol^{-1} above the 1,3-diradical minimum (**C**), whereas on the T_1 surface, the barrier height (**XXVI**) is more than 50 kcal mol^{-1}. Therefore, the rearrangement to cyclopentene is feasible if 1,3-cyclopentanediyl is formed in the S_0 state or if the photodissociation is initiated by a high-energy activation mode. As we have discussed earlier, dissociation via the S_0 state is more likely to occur in the direct photolysis than in the triplet-sensitized photolysis. This explains why some cyclopentene is obtained in the direct photolysis.[3] The observed increase in cyclopentene yield in the higher energy (e.g. laser-jet, 185 nm) photolysis[3,10]

(28) Dervan, P. B.; Dougherty, D. A. In *Diradicals*; Bordon, W. T., Ed.; Wiley: New York, 1982; pp 107−151.

Table 2. Ground and Excited State Energetics for the Potential Energy Surfaces of 1,3-Cyclopentanediyl, Bicyclopentane and Cyclopentene

geometry	state	energy E_h CASSCF (2,2)	energy E_h MP2	rel energy, kcal mol^{-1} (zero pt energy corr)
1,3-cyclopentanediyl S_0 minimum (**C**, Figure S8a)	S_0	−193.9026	−194.5252	0.0
1,3-cyclopentanediyl T_1 minimum (**D**, Figure S8b)	T_1	−193.9041	−194.5330[a]	−4.9
1,3-cyclopentanediyl S_0/T_1 crossing (**XXIV**, Figure S8c)	S_0/T_1	−193.8942 −193.8941		
bicyclopentane (Housane E, Figure S8d)	S_0	−193.9435	−194.5826	−35.4
1,3-cyclopentanediyl S_0 H-shift transition state (**XXV**, Figure S8e)	S_0	−193.8780[†]	−194.4860	24.6
cyclopentene S_0 minimum (**C**, Figure S8g)	S_0	−194.0047[b]	−194.6302	−56.9
1,3-cyclopentanediyl T_1 H-shift transition state (**XXVI**, Figure S8f)	T_1	−194.8208[c] (2482 *i*cm^{-1})	−194.4287	60.6
cyclopentene T_1 minimum (**XXVII**, Figure S8h)	T_1	−193.8904[b]	−194.5088	10.3
cyclopentene S_0/T_1 crossing (**XXVIII**, Figure S8i)	S_0 T_1	−193.8893[b] −193.8884[b]		

[a] The 2 electron triplet is a single configuration ROHF/ROMP2 problem. [b] 4 electron, 4 orbital active space. [c] 4 electron, 3 orbital active space.

is also consistent with our results. On the other side of the S_0 H-shift transition state (**XXV**), we have located an S_0 cyclopentene minimum (**F**, Figure S8g) that lies some 80 kcal mol^{-1} below this transition state. We have also located the T_1 cyclopentene minimum (**XXVII**, Figure S8h) and the cyclopentene S_0/T_1 crossing (**XXVIII**, Figure S8i). However, these are of interest only if the H-migration on the T_1 state is possible.

4. Conclusion

In this work, we have documented the reaction paths for the α C−N and β C−C cleavage that take place during direct and sensitized photolysis of DBH. These reaction paths span the four different potential energy surfaces associated with the S_0, S_1 (n−π*), T_1 (n−π*), and T_2 (π−π*) states. Our computational results provide information on the mechanism of these photoreactions in terms of ground- and excited-state intermediates, transition structures, and "funnels" where the excited-state species can decay to lower lying states via IC or ISC.

Our results show that the "unknown" excited-state region indicated in Scheme 1 comprises three excited-state species. Two of these species (corresponding to structures **XV** and **XX**) are singlet (n−π*) and triplet (n−π*), respectively. These species appear to be metastable since little energy is required to prompt their decay via IC and/or ISC. In contrast, the third excited-state intermediate (corresponding to structure **XIX**) has a mixed ^{3}(n−π*)−^{3}(π−π*) electronic structure, and it is the only intermediate capable of (potentially) generating both hydrazonyl biradicals via β C−C cleavage and diazenyl biradicals. This intermediate is also quite stable since its evolution is impaired by a ∼16 kcal mol^{-1} barrier.

The reaction network generated upon transformation and decay of these three excited-state intermediates is rather complex (see eq 1). The singlet intermediate **XV** can decay directly to S_0 or undergo ISC to generate the intermediate **XIX** or/and **XX**. On the other hand, the intermediate **XX** can directly decay to the T_1 diazenyl biradical or undergo IC to generate the intermediate **XIX**. In contrast, the much more stable intermediate **XIX** cannot be converted to the other excited state intermediates but can only react via either α C−N or β C−C cleavage. Our computed energetics suggest that **XIX** is the best candidate for the experimentally observed transient triplet intermediates. On the other hand the species **XV** and **XX** must be short-lived as indicated in Scheme 2a.

Direct photolysis leads to three competing processes. The first is the α C−N scission (ring-opening) on the S_1 surface over a small barrier leading to S_0 diazenyl biradicals with subsequent denitrogenation. It is also possible for the singlet excited molecule to undergo ISC to the T_2 state, followed by efficient IC to form a triplet intermediate. These intermediates can subsequently undergo either α C−N or β C−C cleavage, although the activation barrier for β C−C scission in unsubstituted DBH seems too high to compete effectively with α C−N breakage.

The fate of a photoexcited molecule in triplet-sensitized photolysis should depend on which of the two triplet states, ^{3}(n−π*) and ^{3}(π−π*), are populated. However, our computations reveal the existence of a T_1/T_2 (i.e. ^{3}(n−π*)/^{3}(π−π*)) funnel not far from the Franck−Condon region which can, in principle, interconvert these states. Thus if the (π−π*) state is initially populated in the Franck−Condon region, the system may decay directly to the more stable triplet intermediate **XIX** or generate triplet diazenyl biradicals via formation of the triplet (n−π*) intermediate **XX**. If the (n−π*) state is populated, then there again will be a competition between α C−N and β C−C cleavage reactions due to the two possible decay routes of the initially formed intermediate (n−π*) **XX**.

The relative activation energies for α and β cleavage from the intermediate **XIX** depend on the substituents. Our UHF computations on unsubstituted DBH and the fused DBH derivative show that in the substituted DBH, the "twisting" about the C−N═N−C bridge is reduced by enhanced molecular rigidity. Thus, the effect of the substituents is to increase the ease of coupling between electrons in the π orbital on the N atom and the one in the σ orbital on the β C atom thereby enhancing the stability of the resulting biradical. This explains why azirane becomes a dominant product during the triplet-sensitized photolysis of some fused DBH derivatives such as *anti*-hexahydro-1,4:5,8-dimethanophthalazines. As described above, the rearrangement to azirane following the β C−C cleavage depends partly on the rate of ISC to the ground state (see structure **XXXI,** Scheme 7b). The ISC is favored by the low nuclear velocity of the molecule entering the region of the crossing. This is one factor that may explain why the cyclization to azirane dominates the nitrogen extrusion reaction at lower temperatures.

We have also explored the potential energy surface of the photoproduct of the nitrogen extrusion, namely, 1,3-cyclopentanediyl, cyclopentene, and housane. Our calculation suggests that there is almost no barrier for the ring closure of the singlet 1,3-cyclopentanediyl to form housane while there is a barrier of 24 kcal mol^{-1} for the H migration to form cyclopentene. The energy of the triplet H migration transition state lies more than 50 kcal mol^{-1} above the triplet 1,3-cyclopentanediyl. This is consistent with the fact that the yield of cyclopentene increases when the molecule is excited with the higher energy activation mode such as 185-nm laser photolysis.

Acknowledgment. The authors are grateful to W. Adam and W. Nau for offering many helpful comments on a draft version of this paper. This research has been supported in part by the SERC (UK) under Grant Nos. GR/H94177 and GR/J25123 and by an EU TMR network grant (ERB 4061 PL95 1290, Quantum Chemistry for the Excited State). We are also grateful to NATO for a travel grant (CRG 950748).

Supporting Information Available: Figures S1 to S12 containing structural data for all critical points discussed (23 pages, print/PDF). See any current masthead page for ordering information and Web access instructions.

JA971733V